arXiv:1412.7229v3 [physics.soc-ph] 22 Jul 2015

Navigable Networks as Nash Equilibria of Navigation Games

András Gulyás[1,3], József J. Bíró[1,2], Attila Kőrösi[3], Gábor Rétvári[1,2] & Dmitri Krioukov[4]

[1] High Speed Networks Laboratory, Department of Telecommunications and Media Informatics, Budapest University of Technology and Economics, 2 Magyar tudósok str., Budapest 1117, Hungary.
[2] MTA-BME Future Internet Research Group, Budapest University of Technology and Economics, 2 Magyar tudósok str., Budapest 1117, Hungary.
[3] MTA-BME Information Systems Research Group, Budapest University of Technology and Economics, 2 Magyar tudósok str., Budapest 1117, Hungary.
[4] Northeastern University, Department of Physics, Department of Mathematics, Department of Electrical&Computer Engineering, 360 Huntington Ave, 111 Dana Research Center, Boston, MA 02115, USA.

Abstract

The common sense suggests that networks are not random mazes of purposeless connections, but that these connections are organised so that networks can perform their functions well. One function common to many networks is targeted transport or navigation. Using game theory, here we show that minimalistic networks designed to maximise the navigation efficiency at minimal cost share basic structural properties with real networks. These idealistic networks are Nash equilibria of a network construction game whose purpose is to find an optimal trade-off between the network cost and navigability. We show that these skeletons are present in the Internet, metabolic, English word, US airport, Hungarian road networks, and in a structural network of the human brain. The knowledge of these skeletons allows one to identify the minimal number of edges by altering which one can efficiently improve or paralyse navigation in the network.

Networks are efficient conduits of information and other media. News, ideas, opinions, rumours, and diseases spread through social networks fast, sometimes becoming viral for reasons that are often difficult to predict [1, 2, 68, 4–12]. Many biological networks are also paradigmatic examples of information routing, ranging from information processing and transmission in the brain, to signalling in gene regulatory networks, metabolic networks, or protein interactions [13–16]. Perhaps the most basic example is the Internet whose primary function is to route information between computers. If one is to list some common functions of different networks, then information routing will likely be close to the top. It is thus not surprising that many networks were found navigable, meaning that nodes can efficiently route information through the network even though its global structure is not known to any individual node [17, 18, 69, 20–29].

These findings do not necessarily mean that real networks evolve to become navigable. Navigability can be a by-product of some other evolutionary incentives because different networks have many other different functions as well. In other words, it remains unclear if ideal networks whose only purpose is to be maximally navigable at minimal costs have anything in common with real

networks. Even if they do, then how close are real networks to these ideal maximally navigable configurations? If they are close but not exactly there, or if their navigability suddenly deteriorates, possibly signifying an onset of a disease [30], then what can we do to cure the network and boost its navigability?

Here we show that the ideal maximally navigable networks do share some basic structural properties with the Internet, *E.coli* metabolic network, English word network, US airport network, the Hungarian road network, and a structural network of the human brain. Yet these ideal networks are not generative models of the real networks, where by generative models we mean function-agnostic models that simply try to reproduce some structural properties of real networks. Instead these ideal networks identify minimal sets of edges that are most critical for navigation in the real network. In other words, they are navigation skeletons or subgraphs of real networks. We find that the considered real networks contain high percentages, exceeding 90% in certain cases, of edges from their navigation skeletons, while the probability of such containment in randomized null models is exponentially small. The knowledge of these skeletons allows us to quantify exactly what connections the considered real networks lack to be maximally navigable, and which of their connections are not exactly necessary for that. To define and construct these maximally navigable network skeletons we employ game theory.

Game theory is a standard tool to study the behaviour of a population with given incentives. The population members are called players, and their possible actions are strategies, while cost functions or payoffs express players' incentives. The purpose of a player is to minimise her costs (or maximise her payoffs) by adjusting her strategy. A Nash equilibrium is a game state such that no player can further reduce her costs by altering her strategy unilaterally. Such equilibrium states are local optima where the game can eventually settle after some transient dynamics. The global optimum is an optimum where the total cost of all players is minimised. Since the inception of game theory a broad palette of games has been introduced, modelling diverse properties of real-life situations [31], Figure 1.

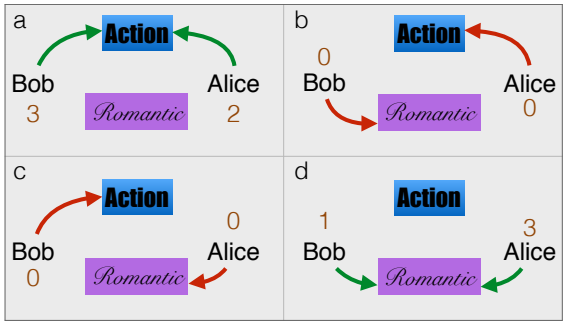

Figure 1: Illustration of game theory. Alice and Bob are happy only if they go out to the movies together, but the level of their happiness depends on what movie they watch. The basic notions of a game: Players: Alice and Bob; Strategies: Go to see an action or a romantic movie; Payoffs: The level of happiness $0, 1, 2, 3$; Nash equilibria: situations in which the players cannot be happier by unilaterally modifying their strategies. In the figure, states (a) and (d) are equilibria when Alice and Bob go together to watch a movie. State (a) is the global optimum since the total happiness $3 + 2 = 5$ is maximised.

Here we use game theory to find the structure of networks that are Nash equilibria of a network

construction game [31–37] with navigability incentives. The concept of Nash equilibrium captures the idea of self-organisation, i.e., of the emergence of structures from the local interaction of rational but selfish players, in contrast with global optimisation used in centralised planning of globally optimal navigable structures [38]. In our Network Navigation Game (NNG), players are network nodes whose optimal strategy is to set up a minimal number of edges to other nodes ensuring maximum navigability. That is, the cost function reflects trade-offs between the number of created edges and navigability. If each node connects to each other node, then this construction is maximally navigable but maximally expensive, too. If no edges are set up, then the cost is zero, but so is navigability. There is a sweet spot of the least expensive but still 100%-navigable network, defined as the network in which all pairs of nodes can successfully communicate using geometric routing [39]. The goal of our game is to find this sweet spot.

Results

The network construction game that we employ is very general and applies to any set of points in any geometry. The latent geometry of numerous real networks is not Euclidean but hyperbolic as shown in [78]. Specifically, the model in [78] extends the preferential attachment mechanism of network growth by observing that in many real networks the probability of establishing a connection depends not only on popularity of nodes, i.e., their degrees, but also on similarity between nodes. Similarity is modeled in [78] as a distance between nodes on the simplest compact space, the circle. The connection probability thus depends both on node degrees (popularity) and on the distance between nodes on the circle (similarity). The node degrees are then mapped to radial coordinates of nodes, thus moving nodes from the circle to its interior, the disk. One can then show that the resulting connection probability depends only on the hyperbolic (versus Euclidean) distance between nodes on the disk, and that the resulting graphs are random geometric graphs [41] growing over the hyperbolic plane. As shown in earlier work [42], these graphs are maximally random, i.e., maximum-entropy graphs that have power-law degree distributions and strong clustering. In other words, power-law degree distributions, coupled with strong clustering, are manifestations of latent hyperbolic geometry in networks. If this geometry is not hyperbolic but Euclidean, then the resulting random geometric graphs still have strong clustering, but their degree distributions are Poisson distributions that do not have any fat tails [41]. The model in [78] has been validated against long histories of growth of several real networks, predicting their growth dynamics with a remarkable precision. It is then not surprising that as a consequence the same model also reproduces a long list of structural properties of these networks [78].

Random geometric graphs [41] are defined as sets of points sprinkled uniformly at random over a (chunk of) geometric space. Every pair of points is then connected if the distance between the points in the space is below a certain threshold. Given that the latent space of real scale-free networks is hyperbolic, our starting point is the first part (uniform sprinkling) of the random geometric graph definition. That is, we first randomly sprinkle a set of points over a hyperbolic disk. We then do not proceed to the second part of the random geometric graph definition. Instead, given only the coordinates of sprinkled nodes, we identify the sets of edges, ideal for navigation, that correspond to the Nash equilibria of our NNGs. We then analyse the structural properties of the resulting ideal-navigation networks, and find that, surprisingly, they also have power-law degree distributions and strong clustering. This result invites us to investigate if these navigation-critical

edges exist in real networks. To check that, we have to know the hyperbolic coordinates of nodes in these real networks in the first place. We infer these coordinates in the considered collection of real networks using the deterministic HyperMap algorithm (Methods). Given only these inferred coordinates, we then construct the ideal-navigation Nash equilibria defined by these coordinates, and compare, edge by edge, the resulting Nash equilibrium networks against the real networks. We find that the real networks contain large percentages of edges from their Nash equilibria. This methodology thus allows us to identify the navigation skeleton of a given real network. We finally check directly that edges in these skeletons are indeed most critical for navigation by showing that their alterations affect drastically network navigability.

Game definition.

We start with a set of players $u = 1, 2, \ldots, N$, i.e., N nodes, scattered randomly over a hyperbolic disk of radius R. The densities of players' polar coordinates (r, ϕ), $r \in [0, R]$, $\phi \in [0, 2\pi]$, are [42]

$$\rho(r) = \frac{\alpha \sinh(\alpha r)}{\cosh(\alpha R) - 1}, \quad \rho(\phi) = \frac{1}{2\pi}, \tag{1}$$

where $\alpha > 1/2$ is a parameter controlling the heterogeneity of the layout. If $\alpha = 1$, the players are distributed uniformly over the hyperbolic disk because the area element at coordinates (r, ϕ) is $dA = \sinh(r)\, dr\, d\phi$. The desired player scattering is achieved in simulations by placing players u at polar coordinates $r_u = (1/\alpha)\,\mathrm{acosh}\,\{1 + [\cosh(\alpha R) - 1]\, U\}$ and $\phi_u = 2\pi U$ where U for each u is a random number drawn from the uniform distribution on $[0, 1]$. The hyperbolic distance between any two players u and v is

$$d(u, v) = \mathrm{acosh}\left[\cosh r_u \cosh r_v - \sinh r_u \sinh r_v \cos(\phi_u - \phi_v)\right]. \tag{2}$$

In greedy geometric routing, player u routes information to some remote player v by forwarding the information to its connected neighbour u' closest to v in the plane according to the distance above. If u has no neighbour u' closer to v than $u$self, then navigation fails, and we say that u cannot navigate to v. The percentage of pairs of players u, v such that u can successfully navigate to v is called the success ratio. If this percentage is 100%, we say that the network is maximally (100%) navigable.

The strategy space of player u is all possible combinations of edges that u can establish to other players. One extremal strategy is to establish no edges. The other extreme is to connect to everyone. The total number of possibilities for u is 2^{N-1}. Any combination of strategies that all players select is a network on N nodes.

The objective of each player u is to set up a minimal number of edges to other players such that u can still navigate to any other player in the network. Formally, the cost function of player u that it minimises is $c_u = k_u + n_u$, where k_u is the number of edges that u establishes, and n_u is either zero if u can navigate to everyone, or infinity otherwise. A more formal description of the strategies and payoffs can be found in Appendix 1.

Nash equilibria of the game.

Given any player u, we call player v's coverage area the set of all points closer to v than to u, Figure 2. Trivially v covers itself, since it is closer to itself ($d(v, v) = 0$) than to u. Therefore if u connects to all other players, then u trivially covers them all. The optimal strategy for u minimising u's costs is thus to connect to a minimal number of players such that the union of their coverage areas contains all the other players. Indeed, if u does that, and if all other players do the same,

then the resulting network is 100%-navigable at minimal number of edges. The network is fully navigable because if u wants to navigate to any remote player w, then by construction there exists u's neighbour v that contains w in its coverage area, and u can use v as the next hop towards w. If v is not directly connected to w, then there exists v's neighbour v' that contains w in its coverage area, so that v can route to v', and so on until the information reaches destination w lying within the intersection of all the coverage areas along the path, Figure 2. The problem of finding the optimal set of edges for u thus reduces to the minimum set cover problem [43]. A formal description of the equilibrium network and a detailed example (for simplicity in the Euclidean plane) can be found in Appendix 2.

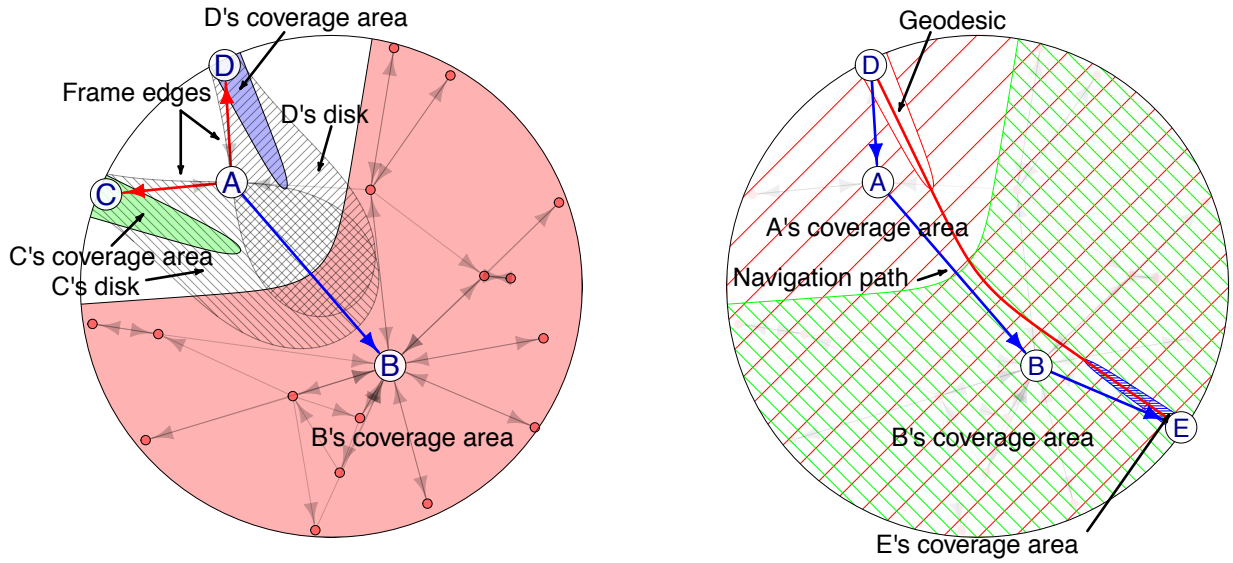

(a) (b)

Figure 2: Illustration of the network navigation game (NNG). Panel (a) shows the optimal set of connections (optimal strategy) of node A in a small simulated network. All nodes are distributed uniformly at random over the hyperbolic disk, and A's optimal strategy is to connect to the smallest number of nodes ensuring maximum (100%) navigability. These nodes are B, C, and D because it is the smallest set of nodes whose coverage areas, shown by the coloured shapes, contain all other nodes in the network. B's coverage area for A (red) is defined as a set of points hyperbolically closer to B than to A, therefore if A is to navigate to any point in this area, A can select B as the next hop, and the message will eventually reach its destination, as the second panel illustrates. Link AC (and AD) in panel (a) is also a frame link, because A is the closest node to C, as illustrated by the hyperbolic disk of radius $|AC|$ centred at C (the line-filled shape), which does not contain any nodes other than C and A. Therefore to navigate to C, A has no choice other than to connect directly to C. Panel (b) shows the sequence of shrinking coverage areas along the navigation path (blue arrows) from D to E. The red curve is the geodesic between D and E in the hyperbolic plane. The coverage areas are shown by the shapes filled with lines of increasing density. The largest is A's coverage for D. The next one is B's coverage for A. The smallest is E's coverage for B.

The Nash equilibrium of this game is not necessarily unique. There can exist different networks minimising the cost defined above. As specified in Appendix 2, in what follows, among all the NNG equilibria, we always select the unique one that minimises the sum of distances span by its edges, thus making the NNG Nash equilibrium network construction deterministic. However there also exist certain edges, which we call frame edges, necessarily present in any Nash equilibrium. Edge $u \to v$ is a frame edge if u is the closest player to v. In this case u cannot navigate to v through any other players since there is no one closer to v than $u$self, so that u must connect directly to v to reach it, Figure 2. If at least one of such edges is absent, the network is not fully navigable. The exact definition of the "frame topology" consisting the frame edges can be found in Appendix 3.

In any Nash equilibrium of this game, each player computes its optimal strategy independently of others. In game theory such equilibria are called dominant strategy equilibria. Moreover the equilibrium is also a social optimum since one cannot create a fully navigable network using less edges.

Structural properties of Nash-equilibrium networks.

Using the trigonometry of overlapping hyperbolic disks, we show in Appendix 4 that if the node density is uniform ($\alpha = 1$), then the probability $p(d)$ that two players u and v located at distance $d \equiv d(u, v)$ are connected in a Nash equilibrium network lies between $\exp(-8\,\delta\, e^{d/2})$ and $\exp(-2\,\delta\, e^{d/2})$,

$$e^{-8\,\delta\, e^{d/2}} \leq p(d) \leq e^{-2\,\delta\, e^{d/2}} \ , \tag{3}$$

where δ is the average density of players on the disk, that is $\delta = N/A$, where A is the disk area. The expected degree of player u at polar coordinates $(r_u, 0)$—we can assume that u's angular coordinate is $\phi_u = 0$ without loss of generality—is then $\bar{k}(r_u) = N \int p[d(u, v)]\, \rho(r_v)\rho(\phi_v)\, dr_v\, d\phi_v$, where $\rho(r_v)$ and $\rho(\phi_v)$ are the player densities from Eq. (1). We can evaluate this integral to find that the expected number $\bar{k}(r)$ of connections of a player at radial coordinate r is bounded by (analytically shown in Appendix 5)

$$\frac{1}{2} e^{(R-r)/2} \leq \bar{k}(r) \leq 2\, e^{(R-r)/2} \ , \tag{4}$$

where $r \equiv r_u$. It then follows that the average degree of players in the network, given by $\bar{k} = \int_0^R \bar{k}(r)\rho(r)\, dr$, lies between 1 and 4,

$$1 \leq \bar{k} \leq 4. \tag{5}$$

We also see from Eq. (4) that the degree of players decays exponentially as the function of their radial position, $\bar{k}(r) \sim e^{-r/2}$, while their density exponentially increases, $\rho(r) \sim e^{r}$, Eq. (1). The combination of these two exponentials yields the power-law degree distribution (see Appendix 6 for the detailed derivation) in the network [44, 45]

$$P(k) = \frac{1}{k!} \int_0^R e^{-\bar{k}(r)} [\bar{k}(r)]^k \rho(r)\, dr = 2 \left(\frac{\bar{k}}{2}\right)^2 \frac{\Gamma(k-2, \bar{k}/2)}{k!} \sim k^{-3}. \tag{6}$$

We also show analytically in Appendix 7-8, that the average clustering $\bar{c}(k)$ of players of degree k decays with k as $1/k$, while the average clustering $\bar{c} = \sum_k P(k)\bar{c}(k)$ in the network is around 0.45, also confirmed in simulations. Clustering does not depend on network size or average degree, meaning that clustering is a positive constant even in the large graph size limit. Remarkably, neither degree distribution nor clustering depend on the player density δ.

For non-uniform node density $\alpha \neq 1$, we can analytically obtain only the lower bound for $\bar{k}(r, \alpha)$, which is still proportional $e^{-\frac{r}{2}}$, i.e., independent of α if $\alpha > 1/2$, Appendix 9. This lower bound suggests that the degree distribution is a power law $P(k) \sim k^{-\gamma}$ with exponent $\gamma = 2\alpha + 1$, which we confirm in simulations in Appendix 9. Figure 3 shows that the closer the γ to 2, the stronger the clustering, the cheaper the network, and the more efficient and robust the navigability. The value of $\gamma = 2$ thus appears as the "best choice" for a network—the network is maximally navigable at the lowest cost. These results complement existing works [46, 23] showing that $\gamma = 2$ yields most navigable networks, by adding that this γ also provides a minimum cost equilibrium topology as well, explaining the emergence of these networks from the interaction of selfish players.

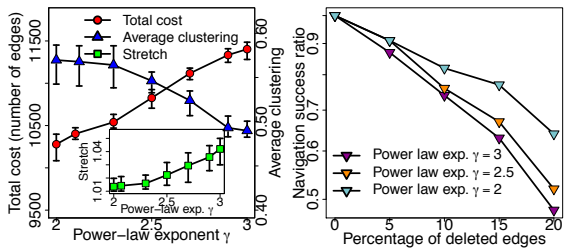

(a) (b)

Figure 3: Topological properties of NNG equilibrium networks as a function of the power-law exponent. Panel (a) shows the total cost (number of edges), average clustering $\bar{c}$, and stretch in NNG-simulated networks as functions of γ. Stretch (shown in the inset) is the average factor showing by how much longer the greedy navigation paths are, compared to the shortest paths in the network. Stretch equal to 1 means that all navigation paths are shortest possible. The plotted points are mean values while the error bars show minimum and maximum values obtained for the NNG over 10 random sprinkling of nodes for a given value of γ. Panel (b) shows the success ratio as a function of the percentage of edges randomly deleted from the network. The smaller the γ, the more robust the navigability with respect to this network damage.

Figure 4 and Table 1 confirm our analytic results and shows that some basic structural properties of NNG-simulated networks are similar to some real networks.

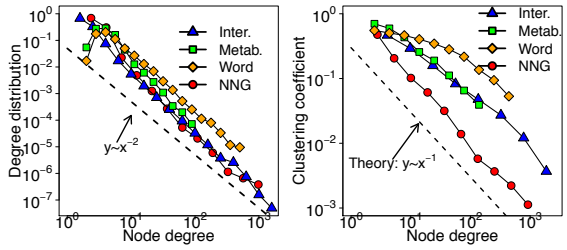

(a) (b)

Figure 4: NNG equilibrium networks share basic structural properties with real networks. The real networks considered are the Internet, metabolic reactions, and the English word network, see Methods. Panel (a) and (b) shows the degree distribution and the average clustering coefficient of nodes of a given degree in the real and NNG networks. The dashed black lines are the power laws with exponents -2 and -1. The power law decay of the clustering coefficient for the NNG is shown analytically in Appendix 7. The clustering coefficient of a node of degree k is the number of triangular subgraphs containing the node, divided by the maximum possible such number, which is $k(k-1)/2$. In the NNG network, the disk radius is $R = 21.2$ and $\alpha = 0.5$. There are no other parameters.

Network	Inter.	Metab.	Word	NNG
Nodes	23748	602	4065	5000
Edges	58414	2498	38631	7955
Avg. deg.	4.92	8.29	19.01	3.18
Avg. clust.	0.61	0.55	0.45	0.60
Avg. dist.	3.52	3.22	2.43	3.89
Diam.	10	6	6	10

Table 1: Comparison of basic structural properties of real and NNG networks. The average distance and diameter are the average and maximum hop lengths of the shortest paths in the network. The average degree in the NNG-simulated network is lower than in the real networks because the NNG generates navigable networks with minimum numbers of edges. In the NNG network, the disk radius is $R = 21.2$ and $\alpha = 0.5$. There are no other parameters.

Our results also suggest that the incentive for navigability alone may be sufficient to explain the properties of complex networks to a certain degree. Yet we cannot really make this claim based only on such large-scale statistical similarities. A more detailed link-by-link comparison between real and corresponding NNG networks is needed to understand how well the NNG reflects reality.

Network Navigation Game versus real networks.

Figure 5 and Table 2 show the results of this analysis applied to these and other real networks.

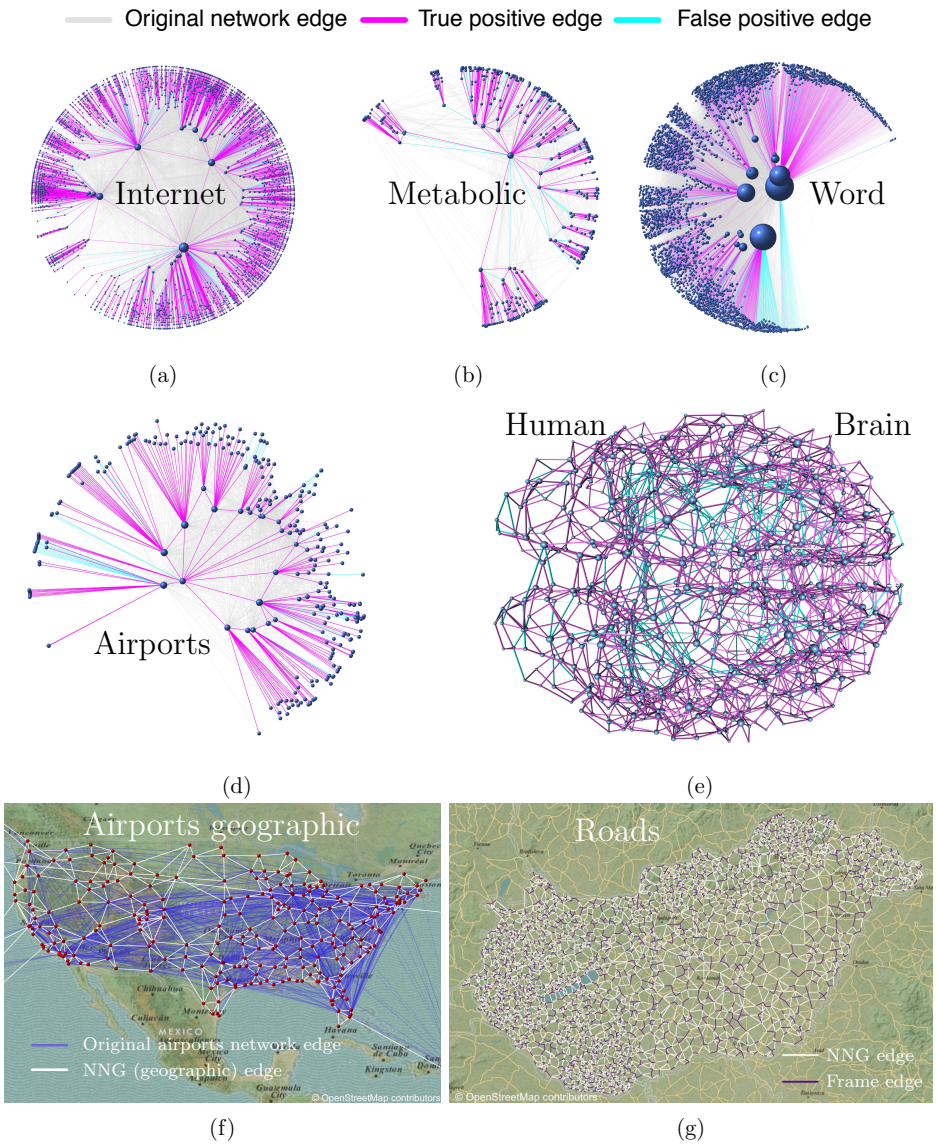

Figure 5: Network Navigation Game (NNG) predicts well links in real networks. Panels (a), (b), and (c) visualise the Internet, metabolic, and word networks mapped to the hyperbolic plane as described in the Methods section. The hyperbolic coordinates of nodes are then supplied to the minimum set cover algorithm that finds a Nash equilibrium of the NNG for each network. Panels (d) and (e) do the same for the US airport network and for the human brain, except that in the brain the physical coordinates of nodes are used. The grey edges are present in the real networks but not in the NNG networks. These edges may exist in real networks for different purposes other than navigation, so that the NNG can say nothing about them. The false positive turquoise edges are present in the NNG networks but not in the real networks. The true positive magenta edges are present in both networks. Panels (f) and (g) show the NNG equilibrium network based on the physical (geographic, versus hyperbolic) coordinates of US airports, and the NNG network for the Hungarian road network. The NNG networks have the same sets of nodes as the corresponding real networks, but the sets of edges are different. For visualisation purposes the grey edges are suppressed in the human brain and Hungarian road networks. The detailed statistics of edges are in Table 2. The cartography in the background of panels (f) and (g) are licensed as CC BY-SA (see www.openstreetmap.org/copyright for details).

	Inter. H	Metab. H	Word H	Roads E	Airp. S	Airp. H	Brain E
Nodes	4919	602	4065	3136	283	283	998
Real edges ($\|R\|$)	28361	2498	38631	-	1973	1973	17865
NNG edges ($\|M\|$)	5490	743	4634	9808	643	328	2591
True positives ($\|T\|$)	4556	643	3311	8776	65	277	2306
False positives ($\|F\|$)	934	100	1323	1032	578	51	285
Precision ($\|T\|/\|M\|$)	83%	87%	71.5%	89.48%	10.1%	84%	89%
Frame edges ($\|M_F\|$)	3680	415	3304	3105	199	249	716
Frame true positives ($\|T_F\|$)	3243	378	2528	2931	15	216	677
Frame prec. ($\|T_F\|/\|M_F\|$)	88%	91%	77%	94.40%	7.5%	87%	94.6%
Navigation success ratio	87%	85%	81%	-	54%	89%	89%

Table 2: The table quantifies the relevant edge statistics in Figure 5, showing the total number of edges in the real networks $|R|$, and in their NNG equilibrium networks $|M|$, the number of true positive (magenta edges in Figure 5) $|T|= |M \cap R|$, the number of false positive (turquoise edges in Figure 5) $|F|= |M \setminus R|$, and the true positive rate, or precision, defined as $|T|/|M|$. The precision statistics is also shown for the frame edges. Capital letters H,E,S after the network names refer to the embedding geometry: H:hyperbolic, E:Euclidean, S:spherical. The Euclidean coordinates in the brain are three-dimensional.

We cannot expect real networks to be identical to NNG networks because the latter are minimum-cost maximum-navigation idealisations, while each individual real network performs many other functions different from navigation. In particular, since real networks must be error-tolerant and robust with respect to different types of network damage, we expect the number of edges in real networks to be noticeably larger than in their minimalistic NNG counterparts—something we indeed observe in Table 2. Yet if navigation efficiency does matter for real networks, then we should expect a majority of edges present in these NNG idealisations to be also present in the corresponding real networks. Table 2 confirms these expectations as well. The NNG precision in predicting links in real networks, defined as the ratio of NNG true positive links to the total number of NNG links, exceeds 80% for most networks, while the precision in predicting frame links, crucial for navigation, exceeds 90% for some networks. In Appendix 10 we juxtapose these numbers against the corresponding numbers in randomized null models, where they are exponentially small, upper bounded by 0.1%. We also note that since the real networks have many more links than NNG networks, their navigability may not suffer much from missing a small percentage of NNG links, as confirmed by the success ratio results in the same figure.

Of particular interest to us here are networks that are explicitly embedded in the physical space. In these cases we may not need to embed the network, but use instead the physical coordinates of its nodes to construct the NNG equilibria. We consider three examples: the Hungarian road network, the airport network of the United States, and a structural network of the human brain. In the first network the nodes are the cities, towns, and villages of Hungary, while in the second network the nodes are US airports. Two nodes are linked if they are connected by a direct road or flight. In the brain network the nodes are small regions of average size 1.5cm^2 covering entirely both hemispheres of the cerebral cortex, and two regions are connected if a structural connection between them is detected in diffusion spectrum imaging. We expect the NNG to be particularly accurate in predicting links in these networks using the physical—instead of hyperbolic—coordinates of nodes. We note that these physical coordinates are Euclidean in all the three cases. The embedding space

is two-dimensional Euclidean and spherical space in the road and airport cases, and it is three-dimensional Euclidean space in the brain case. Our method to construct an NNG equilibrium applies without change to any set of points in any geometric space, and the analytic results on the structure of NNG equilibrium networks in Euclidean spaces are in Appendix 11. We apply our method to find the NNG equilibrium networks using the physical coordinates of nodes in these three real networks, and then compare them to their NNG equilibria also in Figure 5 and Table 2.

We observe that in the brain and road networks the NNG link prediction accuracy is particularly high, reaching 89% for all the links and 94-95% for the frame links. For the brain this result implies that the spatial organisation of the brain is nearly optimal for information transfer, in agreement with previous results [47–50]. In the Hungarian road network, nearly all frame links, crucial for efficient navigation using geography, are present. Practically this means that Hungarians have luxury to go on a road trip without a map since all the major roads required by geographic navigation are there, albeit the condition of some of those roads is not as luxurious. To put it simply, there are roads where people with a compass may think they should be.

For the US airport network however, the geographic results are poor. These poor results may be unexpected at first, but they have a simple explanation in that the geometry of the airport network is not really Euclidean, as the geometry of the nearly planar road network, but hyperbolic. Indeed, efficient paths in the airport network optimise not so much the geographic distance travelled, but the number of connecting flights. As a consequence, most paths go via hubs. As opposed to the road network, where the number of roads meeting at an intersection does not vary that much from one intersection to another, the presence of hubs in the airport network makes the network heterogeneous, i.e., node degrees vary widely. This heterogeneity effectively creates an additional dimension (the "popularity" dimension in [78]). That is, in addition to their geographic location, airports also have another important characteristic—the size or degree. This extra dimension makes the network hyperbolic [42]. The NNG results for the hyperbolic map of the airport network in Figure 5 are as good as for the other networks.

How to cure or injure a network efficiently.

The knowledge of the NNG equilibrium of a given real network makes it possible to efficiently identify links that are most critical for navigation in the network. Since NNG equilibrium networks are maximally navigable networks composed of the smallest number of links, we expect that if we alter a real network by either adding or removing a relatively small number of links belonging to the NNG equilibrium of the network, then such network modifications may significantly affect network navigability.

Figure 6 supports these expectations. In the figure, we take the considered real networks, and add to them certain numbers of links that are present in the NNG equilibria of the real networks, but not present in the networks themselves. About 1-2% of added edges, compared to the original numbers of edges in the networks, increase network navigability significantly, while the addition of 2-5% of edges makes all the networks 100%-navigable. Similarly, the targeted removal of a small portion (1-5%) of edges belonging both to the NNG equilibria of the networks, and to the network themselves, degrades network navigability by 10-30%.

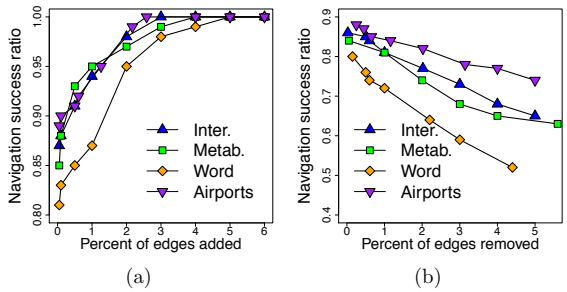

Figure 6: NNG equilibria of real networks helps to improve or degrade their navigability. The edges from the NNG equilibria of the considered real networks are first sorted in the decreasing order of betweenness centrality, and then either added to the real network if not already there (panel (a)), or removed from the network if present (panel (b)). The x-axis shows the percentage of added or removed edges compared to the number of edges in the original real network. Navigation success ratio is computed as the number of node pairs between which geometric routing is successful divided by the number of all node pairs.

Discussion

We emphasise that the considered Nash equilibrium networks are minimalistic idealisations, concerned only with maximising the efficiency of the navigation function at minimal cost (number of links). Reality differs from this ideal in many ways. First, real networks must be robust with respect to noise and random failures. This robustness requirement explains why the considered real networks have strictly more links that their Nash equilibria. Maximum navigability can obviously be achieved not only at the minimal cost, but also at a higher cost. Second, transport processes in real networks are also noisy, and can follow not only steepest descent path (greedy navigation), but also any downstream paths, still achieving 100% reachability. Yet the noisier the transport process, the less likely it stays to the shortest path, leading to higher stretch and longer travel times, thus degrading navigation efficiency in terms of these parameters. Third, navigability does not always have to be maximised as many specific networks perform many specific functions other than navigation. Our game-theoretic approach can be extended to accommodate some of these functions, such as error tolerance or policy compliance [51], but not all possible functions of different real networks can be formalised within this game-theoretic framework. Some networks are centrally designed to optimise a particular function globally [38]. Game theory is not needed to formalise such global optimisation strategies. It is more suited for self-organised networks, in which each node behave selfishly according to its own incentive, independent of other nodes. In other words, Nash equilibrium networks are structural manifestations of local incentives of nodes for efficient transport or communication, in contrast with existing generative or optimisation models of complex networks [52, 53]. Finally, all real networks are dynamic and growing, while Nash equilibria correspond to static network configurations. However it has been recently shown [54] that in case of random geometric graphs—to which the considered Nash equilibrium networks effectively belong according to the results in Appendix 12—one can map an equilibrium network model to an identical growing one.

Notwithstanding these limitations we have shown that ideal networks designed to be maximally

navigable at minimal cost share basic structural properties with real networks. Compared to existing works on navigation-optimal distributions of shortcut edges in Euclidean grids [55–58] which do not yield realistic network topologies, this result is quite unexpected because there is absolutely nothing in the definition of these ideal networks that would enforce or even welcome a formation of any particular network structure. The networks are defined purely in terms of navigation optimality. The surprising finding that the structure of these ideal networks is similar to the structure of real networks should not be misinterpreted as if these idealisations are generative models for real navigable networks. Instead the former are skeletons or subgraphs of the latter. Since these skeletons consist of the minimum number edges required for 100% navigability, there is no even a parameter to control the most basic structural network property—the average degree, which is always controllable in generative models. On the contrary, as follows from Eq. (5), the average degree in these skeletons is uncontrollable and lies between 1 and 4.

We find that if network geometry is hyperbolic, then our navigation skeletons have power-law degree distributions and strong clustering. The values of power-law exponent γ close to 2, observed in many real networks [59, 60], appear as the best possible choice. In this case not only reachability is 100%, but also the network cost and stretch are minimised and navigability robustness is maximised, compared to other values of γ in Figure 3.

These results apply to sets of points in hyperbolic space, but the navigation skeleton construction itself is by no means limited to these hyperbolic settings. It is very general, and applies to any set of points in any geometric space, as illustrated by the brain and road networks where we have used the Euclidean $2d$ and $3d$ physical coordinates of nodes to construct the navigation skeleton of the network. Our finding that the brain contains almost fully its navigation skeleton appears as a mathematically clear and conclusive evidence that the spatial organisation of the brain is nearly optimal for communication and information transfer, corroborating existing work on the subject [47–50].

We note that the connection between the structure and function of networks is often studied in the logically reverse direction: structure→function. That is, first some data about the structure of real networks is obtained, and then questions concerning how optimal this structure is with respect to a given network function are investigated. This logic does provide some evidence that the network might have evolved optimising this function, but this evidence is quite indirect and unreliable compared to the direct demonstration that functionally optimal networks have the structure observed in reality: function→structure. The common sense suggests that this causal direction must reflect reality more adequately since networks, either designed or naturally evolving, do not have a completely random structure but the structure (effectively) optimising some functions. Yet studying networks in this direction is much more challenging primarily because of difficulties in formalising the constraints that a given function imposes, and deriving the resulting optimal network structure. Here, with the help of game theory, we have done so for the navigation function that many real networks (implicitly) perform.

As one would logically expect, the function→structure approach provides a deeper insight into specific details of network's structural organisation that are critical for its functional efficiency. We have confirmed this expectation by demonstrating that our approach can identify links in real networks that are most critical for navigation. A targeted attack on these critical links degrades navigability rapidly, while if a real network is not 100%-navigable, our approach finds the minimal number of not-yet-existing links whose addition to the network boosts up its navigability to 100%. Therefore our approach can be used to identify real network links that should be protected most in

a critical network infrastructure. On the other hand, this approach can also help network designers to prioritise possible link placement options, i.e., pairs of not directly connected nodes, that, if connected, would maximise navigability improvement.

Finally, all the real networks considered here are expected to be navigable. Indeed, the primary functions of the Internet, brain, metabolic, or airport and road networks are to transport information, energy, or people. Semantic and syntactic navigability of word networks is an established fact in cognitive science [61–63]. However one cannot expect all real networks to be highly navigable as navigation is not an important function of every network in the world. In Appendix 13 we consider one example, a technosocial web of trust, in which nodes are public keys of users of a distributed cryptosystem, linked by users' certifications of key-user bindings. There is no reason why this network should be navigable. In agreement with this observation, we then find that this network does not contain a large percentage of edges from its NNG equilibrium, suggesting that the introduced methodology can be also used as a litmus test to investigate if navigation is an important function of a given real network, and if so, then to what degree.

Methods

The real network data. The Internet dataset representing the global Internet structure at the Autonomous System (AS) level is from [64]. The metabolic network is the post-processed network of metabolic reactions in *E. coli* from [78], Snapshot S_1 there. The post-processing details can be found in [78]. The word network is the largest connected component of the network of adjacent words in Charles Darwin's "The Origin of Species" from [65]. The airport network was downloaded from the Bureau of Transportation Statistics `http://transtats.bts.gov/` on November 5, 2011. The structural human brain network and physical coordinates of nodes (regions of interest (ROIs)) in it are the diffusion spectrum imaging (DSI) data from [66].

The hyperbolic maps of real networks. The hyperbolic coordinates of ASes and metabolites are from [64] and [78]. The hyperbolic coordinates of words and airports are inferred using the *HyperMap* algorithm [67]. This algorithm is deterministic, and is based on the growing network model in [78] used to show that the latent geometry of scale-free strongly clustered real networks is hyperbolic. Given an adjacency matrix of a real network, the algorithm infers the hyperbolic coordinates of its nodes by replaying its growth as the model in [78] prescribes. Specifically, the nodes are first sorted in the order of decreasing degrees, and then, starting with the highest-degree node, nodes and their edges are added, one node at a time, to a growing network. The probability, or the likelihood, with which model [78] generates this growing network, depends on the node coordinates. The coordinate of each added node is set by the HyperMap algorithm to the coordinate corresponding to the global maximum of this probability.

The Nash equilibrium networks of NNGs. The hyperbolic or physical, in the airport and brain cases, coordinates are then supplied to the GNU Linear Programming Kit (GLPK) `http://www.gnu.org/software/glpk/` used to find a solution to the corresponding minimum set cover problem. To yield acceptable running times of the solver, the Internet and word networks are reduced in size by extracting their high-degree cores of about 4500 nodes. The Hungarian road data is processed slightly differently. First the cities in Hungary are mapped to their geographic coordinates using the database in `http://www.kemitenpet.hu/letoltes/tables.helyseg_hu.xls`. Then these coordinates are used in the GLPK to find the NNG equilibrium. Each edge in

this equilibrium network is then checked for existence in the real road network. To check that, the GoogleMaps API `https://pypi.python.org/pypi/googlemaps/` is used to find the shortest path between the two cities connected by the edge. The edge is defined to also exist in the real road network if this shortest path does not go via any other city.

Acknowledgements

We thank Olaf Sporns for sharing the brain data, and János Tapolcai and Alexandra Aranovich for useful discussions and suggestions. This work was supported by DARPA grant No. HR0011-12-1-0012; NSF grants No. CNS-1344289, CNS-1442999, CNS-0964236, CNS-1441828, CNS-1039646, CNS-1345286, CCF-1212778 and Hungarian Scientific Research Fund (grant No. OTKA 185101); and by Cisco Systems. G.R. was supported by the OTKA/PD-104939 grant and J.J.B. was supported by the Inter University Centre for Telecommunications and Informatics (ETIK), Hungary.

Appendix 1 - Formal definition of the Network Navigation Game (NNG)

Strategies. The strategy space for a player $u \in \mathcal{P}$ is to create some set of arcs to other players in the network: $S_u = 2^{\mathcal{P}\setminus\{u\}}$. Let s be a strategy vector: $s = (s_0, s_1 \dots s_{N-1}) \in (S_0, S_1 \dots S_{N-1})$ and $G(s)$ be the graph defined by the strategy vector s as $G(s) = \bigcup_{i=0}^{N-1}(i \times s_i)$.

Payoff. The objective of the players is to minimise their cost which is calculated as:

$$c_u = \sum_{\forall u \neq v} d_{G(s)}(u, v) + |s_u|, \quad u, v \in \mathcal{P} \tag{1}$$

where

$$d_{G(s)}(u, v) = \begin{cases} 0 & \exists\, u \to v \text{ greedy path in } G(s) \\ \infty & \text{otherwise.} \end{cases}$$

Appendix 2 - NNG equilibrium

The Nash equilibria of the Network Navigation Game can be characterised for each player independently as follows: take a player u, and for all $v \in V \setminus u$ let $\mathbb{S}_v^u = \{w | d(v, w) < d(u, w)\}$. Trivially $\mathbb{S}_v^u \subset V$ and $\bigcup_{v \in V \setminus u} \mathbb{S}_v^u = V$. The optimal strategy s_u^{opt} of u is the minimal set cover of V with the sets $\mathbb{S}_v^u$, independently from the strategies of the other players. This means that $s = (s_1^{\text{opt}}, s_2^{\text{opt}} \dots s_{N-1}^{\text{opt}})$ is both a NE and a social optimum.

The Nash equilibrium is not necessarily unique as there can exist different solutions of the above set cover problem. In our work we concentrate on a specific equilibrium, which besides being a solution, it also minimises the sum of edge the edge lengths all over the network. This is fully in line with the edge-locality principle of complex networks [68] [69] [70] which many times accounted for the high clustering coefficient. More formally, from the strategy vectors constituting a Nash equilibria s_i and the corresponding graphs $G(s_i) = \bigcup_{i=0}^{N-1}(i \times s_i) = (V, E_i)$ we seek for the one

minimising $\sum_{j \in E_i} d(E_i(j))$.

An example

As an example, let us compute the Nash equilibrium topology for four points in the Euclidean plane A, B, C, D (see Figure 7). Any node u out of these four needs to have a greedy next hop towards

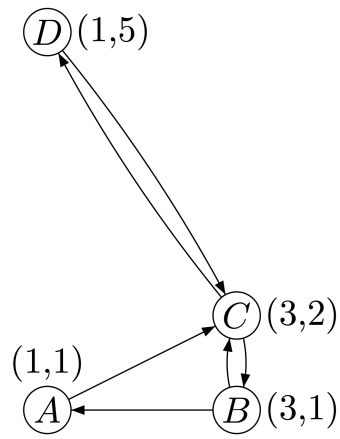

Figure 7: Network Navigation Game in the Euclidean plane.

any other nodes (to avoid infinite cost), while having its number of edges minimised. Note that having a greedy next hop is sufficient since all the other nodes will have greedy next hops towards any other nodes for ensuring $c_u \leq \infty$. This will imply greedy paths between arbitrary pairs of nodes.

Let us compute the sets $\mathbb{S}_v^u = \{w | d(v, w) < d(u, w)\}$ for the nodes, where $d(x, y)$ is the Euclidean distance and the minimal set covers for each node to get the Nash equilibrium.

- $\mathbb{S}_A^B = \{w | d(A, w) < d(B, w)\} = \{A, D\}$, which means that A is a good greedy next hop towards A and D for B, similarly $\mathbb{S}_C^B = \{C, D\}$, $\mathbb{S}_D^B = \{D\}$ therefore the minimal cover for B is {A,C} so B creates two edges to A and C
- $\mathbb{S}_B^A = \{B, C\}$, $\mathbb{S}_C^A = \{C, B, D\}$, $\mathbb{S}_D^A = \{D\}$ therefore the minimal cover for A is {C} so A creates one edge to C
- $\mathbb{S}_A^C = \{A\}$, $\mathbb{S}_B^C = \{B, A\}$, $\mathbb{S}_D^C = \{D\}$ therefore the minimal cover for C is {B,D} so C creates two edges th B and D
- $\mathbb{S}_A^D = \{A, B, C\}$, $\mathbb{S}_B^D = \{B, C, A\}$, $\mathbb{S}_C^D = \{C, B, A\}$ therefore the minimal cover for D is for example {C} (A and B would be also good) so D creates one edge to C

Thus we can construct the graph from these minimal set coverings see Figure 7. This is a Nash equilibrium and a social optimum as there are no lower cost equilibria or state for this game.

Appendix 3 - Frame topology

There exists a well defined "frame topology" G_{frame} with scale-free out-degree distribution which is present in *every* Nash equilibrium, or social optimum of the NNG ($G_{\text{frame}} \subset G(s^*)$) and other possible games having navigation as an incentive ($p_s = 1$). In other words the frame topology serves as a skeleton of any equilibrium topology emerging from navigational games. The frame topology is defined as:

Definition 1 (Frame topology) *Let* $G_{\text{frame}} = \bigcup_{u=0}^{N-1}(u \times g_u)$*, where* $g_u = \{v | v \notin s_u \Rightarrow c_u = \infty\}$.

Practically, the arc (u, v) is contained in G_{frame} if and only if the $d(u, v)$-disk centred at v does not contain any player other than u (see Figure 8). This means that u cannot reach v by greedy

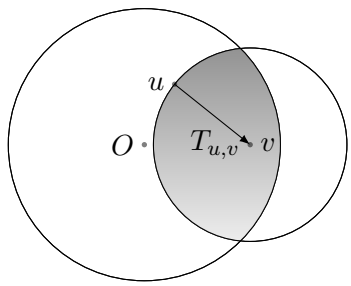

Figure 8: An edge in the G_{frame}

routing through any other players then v, and so it must create an arc towards v to avoid of having infinite cost. Note that the in-degree of each player in G_{frame} will be exactly one.

Appendix 4 - Connection probability

Here we cast the problem in statistical terms. We estimate the percentage of pairs of nodes located at a given distance that are connected in the NNG equilibrium. We call this percentage the effective connection probability. First the connection probability of the Frame Topology is derived. This connection probability is a lower bound for the connection probability in the NNG equilibrium network because the Frame Topology is contained in every NNG equilibrium network. A direct upper bound of the connection probability is also studied. Based on a statistically equivalent lower bound and the direct upper bound, a general formula for the connection probability is induced, in which the average degree of the network is implicitly encoded. This makes it possible to approximate the connection probability (and all other quantities defined by it) using the observed average degree in the NNG simulation.

Connection probability in the Frame Topology

As presented in Appendix 3 an arc (u, v) in the Frame Topology is established if and only if there are no other points (players) within the intersection of the $v-$centred disk with radius $d(u, v)$, and the original disk with radius R. The probability of this event is

$$\left(\frac{T_R - T_{uv}}{T_R}\right)^{N-2} \approx e^{-\delta T_{uv}} \tag{2}$$

An approximation for T_{uv} is as follows: T_{uv} is apparently equals to $2\pi(\cosh d_{uv}-1)(\approx \pi e^{\frac{d_{uv}}{2}}$ for not so small $d_{uv})$ when the $d_{uv}-$disk is completely inside the $R-$disk. On contrary, if $R-r_v < d(u,v)$ (there is real intersection) then much less evidently T_{uv} is approximately $T_{uv} \approx 4e^{\frac{d_{uv}}{2}} e^{\frac{R-r_v}{2}}$. In Figure 9 two characteristic cases are depicted when there is real intersection of the d_{uv}-disk and the R-disk. Let the polar coordinates of node v be (r_v, ϕ_v), and of node u be (r_u, ϕ_u). Let $\phi = |\phi_u - \phi_v|$.

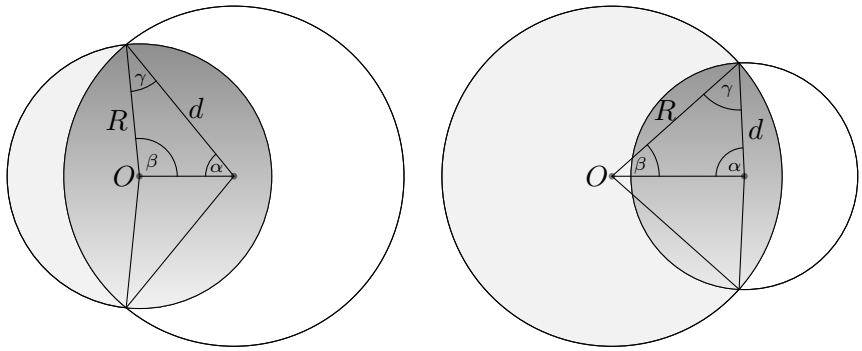

Figure 9: Illustration for T_{uv}

The area T_{uv} is the function of r_u, r_v, ϕ, and R, and can be calculated as the sum of the two circle sectors with angle 2α, radius d_{uv} and angle 2β radius R, and minus the area of the two triangles with angles α, β, γ. That is

$$T_{uv} = 2\beta\left(\cosh(R)-1\right) + 2\alpha\left(\cosh(d_{uv})-1\right) - 2\left(\pi-\alpha-\beta-\gamma\right) \ . \tag{3}$$

where the angles and d_{uv} are given by the hyperbolic law of cosines, however, here the following simpler approximations are used (which are accurate enough when r_u and d_{uv} appear in exponents):

$$d_{uv} \approx R + r_v + 2\ln\frac{\beta}{2} \Rightarrow \beta \approx 2e^{\frac{d_{uv}}{2} - \frac{R+r_v}{2}} \tag{4}$$

$$R \approx d_{uv} + r_v + 2\ln\frac{\alpha}{2} \Rightarrow \alpha \approx 2e^{-\frac{d_{uv}}{2} + \frac{R-r_v}{2}} \ . \tag{5}$$

Applying (3) with neglecting the triangle areas, and using $\cosh(R)-1 \approx e^R/2$, $\cosh(d_{uv})-1 \approx \frac{e^{d_{uv}}}{2}$ we get $T_{uv} \approx 4e^{\frac{d_{uv}}{2}} e^{\frac{R-r_v}{2}}$.

In summary:

$$T_{uv} \approx \begin{cases} \pi e^{d_{uv}} & \text{, if } \ 0 < d_{uv} < R - r_v \\ 4e^{\frac{d_{uv}}{2}} e^{\frac{R-r_v}{2}} & \text{, if } \ d_{uv} > R - r_v \ . \end{cases} \tag{6}$$

This T_{uv} approximations are illustrated in Figure 10 for $R = 12$, $r_v = 6$ and $r_v = 8$. Solid lines are the exact T_{uv} calculations based on (3) and exact computations of angles. Note that there is a sharp change on logarithmic scale between the d_{uv}-slope and $d_{uv}/2$-slope around $R - r_v$. The dashed lines are the T_{uv} approximations when $d_{uv} > R - r_v$.

The calculation of the expected degree of node u requires $e^{-\delta T_{uv}}$ in the following double integration:

$$\delta \int_0^R \int_0^{2\pi} e^{-\delta T_{uv}} \mathrm{d}\phi \sinh(r_v) \mathrm{d}r_v \ . \tag{7}$$

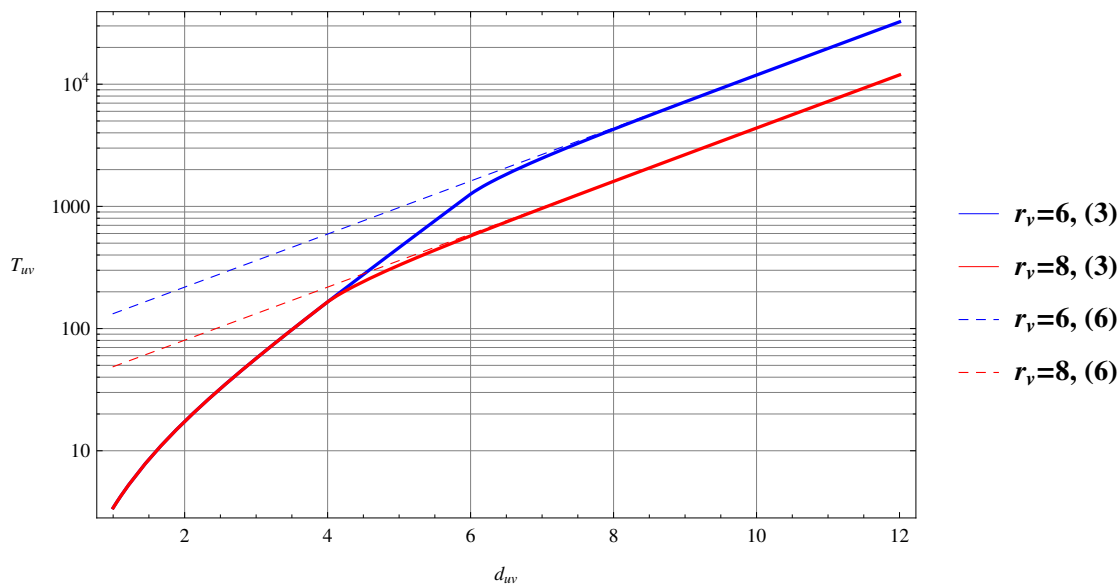

Figure 10: $T_{uv} \approx 4e^{\frac{d_{uv}}{2}} e^{\frac{R-r_v}{2}}$ when there are real intersections (that is when $d(u,v) > 6$ and 4, respectively).

Because the joint expansion of the double integral with respect to r_v and ϕ reveals that the dominant terms will be those in which $d_{uv} > R - r_v$

$$\delta \int_0^R \int_0^{2\pi} e^{-\delta T_{uv}} \mathrm{d}\phi \sinh(r_v) \mathrm{d}r_v \approx \delta \int_0^R \int_0^{2\pi} e^{-\delta 4 e^{\frac{d_{uv}}{2}} e^{\frac{R-rv}{2}}} \mathrm{d}\phi \sinh(r_v) \mathrm{d}r_v \ . \tag{8}$$

Using (4) it can also be shown that

$$\delta \int_0^R \int_0^{2\pi} e^{-\delta 4 e^{\frac{d_{uv}}{2}} e^{\frac{R-rv}{2}}} \mathrm{d}\phi \sinh(r_v) \mathrm{d}r_v \approx \delta \int_0^R \int_0^{2\pi} e^{-\delta 8 e^{\frac{d_{uv}}{2}}} \mathrm{d}\phi \sinh(r_v) \mathrm{d}r_v \ . \tag{9}$$

Therefore,

$$\check{p}(d_{uv}) = e^{-\delta 8 e^{\frac{d_{uv}}{2}}} \tag{10}$$

can be considered as a statistically equivalent connection probability of the Frame Topology and as a latent (a statistically equivalent) lower bound of the connection probability of the equilibrium network of the NNG.

A direct upper bound for the connection probability

An upper bound for connection probability $p(d_{uv})$ can be derived as follows. Let u and v be two points in the R-disk and let $C_{u,v} = \{w | d_{wv} < d_{wu}\}$ denote the area for which v is a good greedy next hop for u. This area is on the side of v bounded by the perpendicular bisector (B_{uv}) of (u,v), see Figure 11. (The figure is in the Poincare model).

Let $A = \{x | C_{u,x} \supset C_{u,v}\}$. If there is a node $w \in A$ then u does not connect to v since it has a node w which covers the whole area that v can and some extra portion of the disk. Putting

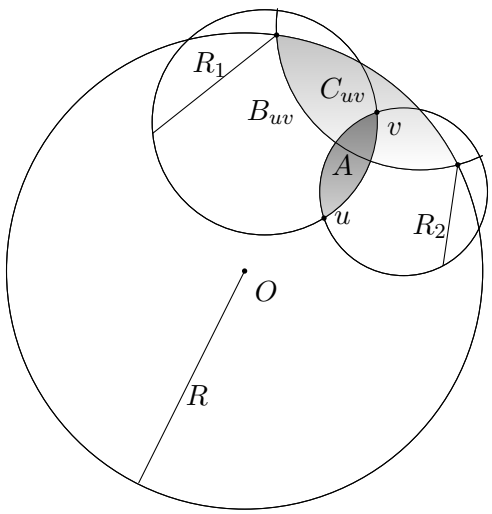

Figure 11: Calculation of $p(d_{uv})$

it differently w can be in the optimal set cover (for u) instead of v. It is easy to see that A is the intersection of two disks with radii R_1 and R_2 (the smaller circles on Figure 11). We can approximate the area of this intersection by the union of two sectors having angles $\phi_1 \approx 2e^{\frac{d_{uv}}{2}-R_1}$ and $\phi_2 \approx 2e^{\frac{d_{uv}}{2}-R_2}$ (by using an approximation on the hyperbolic distance $d_{uv} \approx 2R_i + 2\ln\frac{\phi_i}{2}$) of the R_1 and the R_2 disks respectively. Using this the area of A is given by:

$$T_A \approx \phi_1(\cosh(R_1)-1) + \phi_2(\cosh(R_2)-1) \approx 2e^{\frac{d_{uv}}{2}-R_1}\frac{e^{R_1}}{2} + 2e^{\frac{d_{uv}}{2}-R_2}\frac{e^{R_2}}{2}, \tag{11}$$

which further simplifies to:

$$T_A \approx 2e^{\frac{d_{uv}}{2}}. \tag{12}$$

The probability that there is a node in A is:

$$p(\exists w \in A) = 1 - \left(\frac{T_{\text{disk}} - T_A}{T_{\text{disk}}}\right)^{N-2} \approx 1 - e^{-\delta T_A}, \tag{13}$$

where N denotes the number of nodes and T_{disk} is the area of the R-disk. Trivially $p(d) \leq 1 - p(\exists w \in A)$ so:

$$p(d_{uv}) \leq e^{-\delta T_A}. \tag{14}$$

By substituting T_A we get the following upper bound for the connection probability:

$$p(d_{uv}) \leq e^{-\delta T_A} \approx e^{-2\delta e^{\frac{d_{uv}}{2}}} =: \hat{p}(d_{uv}) \tag{15}$$

A general formula for the connection probability

In the Frame Topology (by definition) every node has exactly one incoming link, hence, the total number of links are N. From this it immediately follows that the average out-degree of Frame

Topology is 1. This will also confirmed by the results of the next note (Appendix 5), in which the conditional expected degree of a node u with radial coordinate r_u is calculated and shown by un-conditioning that the average degree is 1. Regarding the direct upper bound of the connection probability, consider a network in which links are established by this upper bound probability. Also the analysis in the next note implies that the average degree of such a network is 4. Based on the upper (15) and lower (10) bounds and the corresponding average degrees 1 and 4, a general formula of the connection probability can be induced as

$$p(d_{uv}, \delta, \bar{k}) = \mathrm{Exp}\left(-\frac{8}{\bar{k}}\delta e^{\frac{d_{uv}}{2}}\right) . \tag{16}$$

It will be shown in the next sections that a network formed by this connection probability has average degree $\bar{k}$.

This formula is important because if an empirical average degree (which happens to be 2.27) can be observed in experiments (simulations) resulting in equilibrium networks of NNG, then not only upper and lower bounds on the expected degree of a node u and degree distribution, but analytical approximations of them can also be given with this empirical mean. Figure 12 illustrates the relation of the upper and lower bounds, and the approximation of the connection probability to that of simulated NNG.

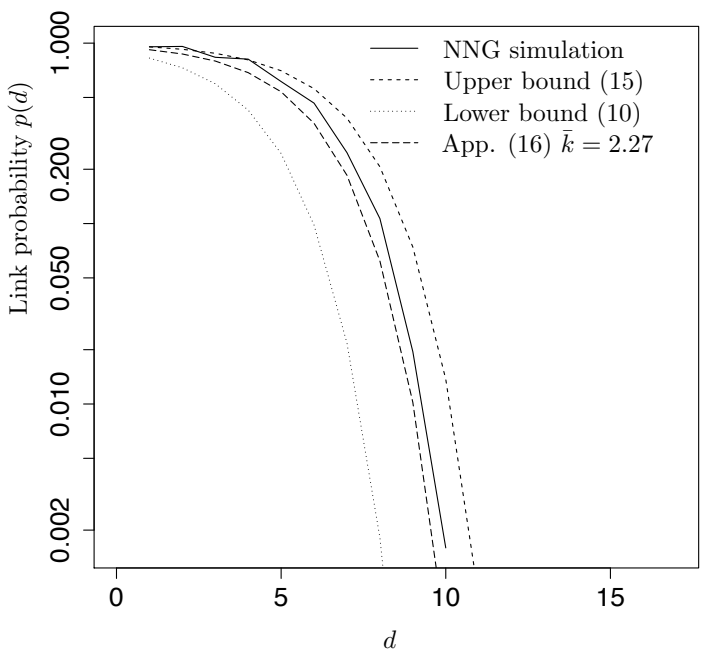

Figure 12: Connection probability as a function of distance in NNG simulations. The figure shows the analytic upper and lower bounds, as well as the analytic approximation with the empirical mean.

Appendix 5 - Expected degree of a given node

The expected (out-)degree of a node u with radial coordinate r_u in a network generated with the effective connection probability formula is given by the following double integral

$$k_{\text{out}}(r_u, \bar{k}, R) = \delta \int_0^R \int_0^{2\pi} p(d_{uv}, \delta, \bar{k}) \mathrm{d}\phi \sinh(r_v) \mathrm{d}r_v \ . \tag{17}$$

The expected node-degree of the equilibrium network of NNG is lower bounded by $k_{\text{out}}(r_u, 1, R)$ (which coincides the expected node-degree of the Frame Topology) whilst $k_{\text{out}}(r_u, 4, R)$ is the upper bound. An analytical approximation with the empirical mean $\bar{k} = 2.27$ can be given by $k_{\text{out}}(r_u, 2.27, R)$.

In what follows a formula is derived for $k_{\text{out}}(r_u, \bar{k}, R)$ based on the integral above. Considering the first integral by ϕ and applying the approximation (consider the hyperbolic law of cosine for d_{uv}, r_u, r_v, $\cosh d_{uv} = \cosh r_u \cosh r_v - \sinh r_u \sinh r_v \cos\phi$)

$$e^{\frac{d_{uv}}{2}} \approx e^{\frac{r_u + r_v}{2}} \sqrt{\frac{1 - \cos\phi}{2}} \tag{18}$$

we get that the integral can be approximated as

$$\delta \int_0^{2\pi} \mathrm{Exp}\left(-\delta \frac{8}{\bar{k}} e^{\frac{d_{uv}}{2}}\right) \mathrm{d}\phi \approx 2\pi\delta(\mathrm{I}(0, x) - \mathrm{S}(0, x)) \approx \frac{1}{2}\bar{k} e^{-\frac{r_u + r_v}{2}} \tag{19}$$

where $x = \frac{8}{\bar{k}}\delta e^{\frac{r_u + r_v}{2}}$ and the last wave due to that $\mathrm{I}(0, x) - \mathrm{S}(0, x)$ (difference of the BesselI and the modified Struve functions) quickly tends to $\frac{2}{\pi}x^{-1}$ as x increases [71]. Now the second integration by r_v gives the expected degree approximation, that is

$$k_{\text{out}}(r_u, \bar{k}, R) \approx \int_0^R \frac{1}{2}\bar{k} e^{-\frac{r_u + r_v}{2}} \sinh(r_v) \mathrm{d}r_v \approx \frac{1}{2}\bar{k} e^{\frac{R}{2}} e^{-\frac{r_u}{2}} \ . \tag{20}$$

One can check that the average degree is indeed $\bar{k}$ with this expected node-degree:

$$\int_{r_u=0}^R \frac{1}{2}\bar{k} e^{\frac{R}{2}} e^{-\frac{r_u}{2}} \frac{\sinh r_u}{\cosh R - 1} \mathrm{d}r_u \approx \frac{1}{6}\bar{k} \operatorname{sech}^2\left(\frac{R}{4}\right)\left(\sinh\left(\frac{R}{2}\right) + 2\cosh\left(\frac{R}{2}\right) + 1\right) \approx \bar{k} \ . \tag{21}$$

We have numerically studied the accuracy of the approximations above. We have found that the exponential decay of the expected degree of nodes ($k_{\text{out}}(r_u)$) is a good approximation of the numerically evaluated expected degree function for a wide range of node density $\delta \in [10^{-8}, 10^{-2}]$. For example, consider a Frame Topology ($\bar{k} = 1$) with $R = 16.5$, $n = 10000$. In this case $\delta = 2.17 \cdot 10^{-4}$. Figure 13 shows how the expected degree decay is matching the exponential decay.

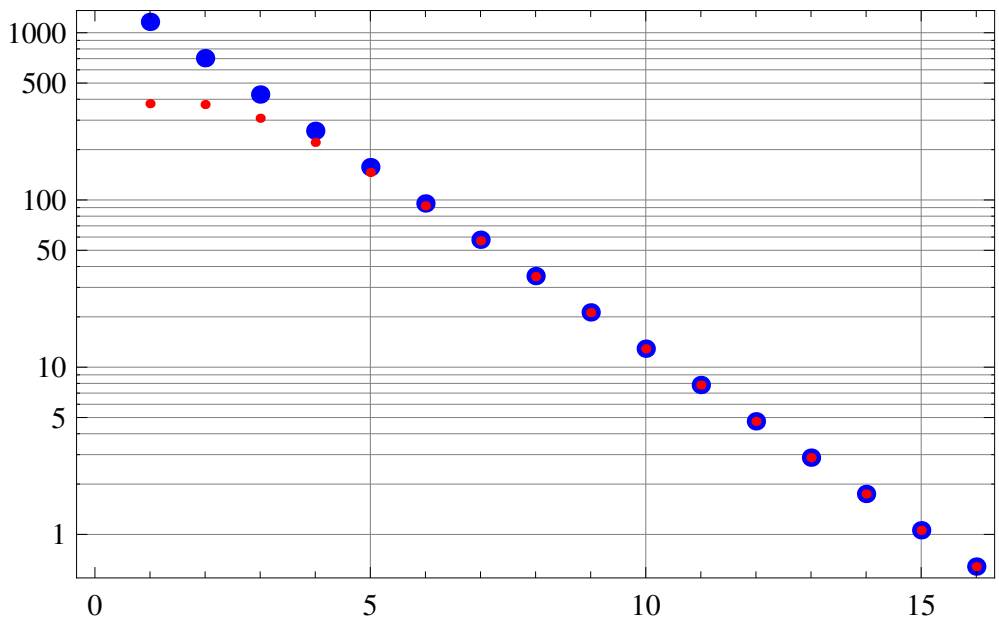

Figure 13: Exponential decay ($C(R)e^{-\frac{r_u}{2}}$, larger blue dots) versus the numerically evaluated exact decay (smaller red dots) of u's expected degree as a function of r_u ($R = 16.5$, $n = 10000$).

We observe that while at smaller r_u there are some approximation errors, for larger values of r_u the match is very good. To quantify further, we note that 99.9% of points have $r_u > 10$ (that is in case of uniformly distributed points on the R(=16.5)-disk, expectedly only about 10 points of the 10000 is inside the disk with radius 10). If we consider the relative errors of the matching one can reveal that for $r_u > 10$ it is smaller than 0.15%, that is for 99.9% of points the expected degree approximation has smaller than 0.15% relative error. To increase the number of points to $n = 30000$ and $n = 50000$ ($\delta = 6.54 \cdot 10^{-4}$, $\delta = 1.08 \cdot 10^{-3}$), the relative error is increasing, especially for smaller values of r_u, but still for 99.9% of the points the relative error smaller than 0.25% and 1%, respectively. If we dramatically decrease the node-density, for example $n = 500$, the relative errors also increase (compared to the $n = 10000$ case), however, it still remains under 0.2% for 99.9% of the points.

Appendix 6 - Degree distribution

Let us recall that in case of uniform distribution of points on an $R-$disk of the hyperbolic plane, the density of the radial coordinates of the points is

$$\rho(r) = \frac{\sinh r}{\cosh R - 1} \tag{22}$$

Note that the expected degree of node u is exponential in the radial coordinate r_u as in [72]. Because of this and the fact that equilibrium network of NNG is also sparse [73] the degree distribution can

be calculated in the same way as in [72] :

$$P(k) = \int_0^R g(k, k_{\text{out}}(r_u))\rho(r_u)\mathrm{d}r_u = \frac{\bar{k}}{2}\frac{\Gamma(k-2, \frac{\bar{k}}{2})}{k!} \tag{23}$$

where $g(k, k_{\text{out}}(r_u))$ is the conditional distribution of the degree of a node with radial coordinate u, and it is Poissonian with mean $k_{\text{out}}(r_u)$ in case of sparse networks. It can also be shown that for larger k

$$P(k) \approx \frac{\bar{k}^2}{2k^3} \ . \tag{24}$$

The direct derivation of the complement cumulant degree distribution from $P(k)$ seems to be intangible, however, from its approximation it can be computed as

$$\bar{F}(k, \bar{k}) \approx 1 - \left(\int \frac{\bar{k}^2}{2k^3}\mathrm{d}k + C\right) \tag{25}$$

where the constant C is 1, and $k \geq \frac{1}{2}\bar{k}$ (in order to have distribution function), that is

$$\bar{F}(k, \bar{k}) \approx \frac{\bar{k}^2}{4}k^{-2} \ , \quad k \geq \frac{1}{2}\bar{k} \ . \tag{26}$$

It is interesting to show that this approximation can also be obtained as the *exact* ccdf of the conditional expected node degrees $k_{\text{out}}(r_u)$. This approximation can be computed as

$$\bar{F}(k, \bar{k}) \approx \int_{r=0}^{r_u(k)} \rho(r)\mathrm{d}r \approx e^{r_u(k)-R} \tag{27}$$

where $r_u(k)$ is the inverse function of $k_{\text{out}}(r_u, \bar{k}, R)$ w.r.t. r_u, i.e.

$$r_u(k) = R - 2\ln\left(2k/\bar{k}\right) \ . \tag{28}$$

Applying this one can obtain the same before as

$$\bar{F}(k, \bar{k}) \approx \frac{\bar{k}^2}{4}k^{-2} \ , \quad k \geq \frac{1}{2}\bar{k} \ . \tag{29}$$

Note that this yields the average degree equal to $\bar{k}$ as expected:

$$\int_{k=\frac{1}{2}\bar{k}}^{\infty} \left(k\frac{\partial(1-\bar{F}(k, \bar{k}))}{\partial k}\right) = \bar{k}. \tag{30}$$

From this, an analytical approximation of the ccdf of the NNG equilibrium network is $\bar{F}(k, 2.27)$, its lower and upper bounds are $\bar{F}(k, 1)$, $\bar{F}(k, 4)$, respectively. In Figure 14 these analytical formulae are drawn also with a completely empirical distribution obtained from NNG simulation.

We also note that the δ-independence of $k_{\text{out}}(r_u)$ and $\bar{F}(k)$ is approximate, but it holds with a high accuracy for $\delta \in [10^{-8}, 10^{-2}]$, including the frame topology.

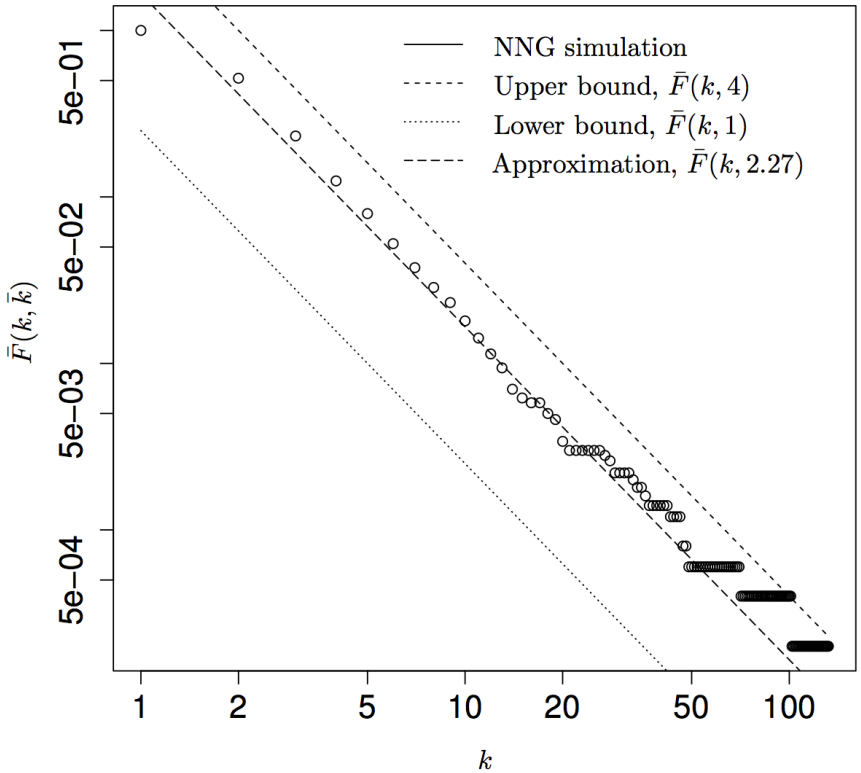

Figure 14: Empirical CCDF of the degree distribution, its analytical upper and lower bounds $\bar{F}(k,4)$, $\bar{F}(k,1)$, and analytical approximation with the empirical mean $\bar{F}(k,2.27)$.

Appendix 7 - Clustering

Here we analyse local clustering using the effective connection probability (16). By means of quasi-symbolic calculations we also show that local clustering depends on the expected node degree k similarly for both lower and upper bounds of the effective connection probability, and that average clustering does not depend on average degree $\bar{k}$.

Let the hyperbolic polar coordinates of the point triplet u, v, w be $(r_u, \phi_u), (r_v, \phi_v), (r_w, \phi_w)$ and $\phi = \phi_u - \phi_v$, $\psi = \phi_u - \phi_w$. The local clustering coefficient $cl(r_u)$ for a given node u is calculated as the ratio of the expected number of link pairs with common edge u and the expected number of link triangles with edge u. For calculating these expected numbers, the joint probabilities of the existence of (u, v) and (u, w) link pair and the existence of the (u, v, w) link triangle are substituted by $p(d_{uv})p(d_{uw})$ and $p(d_{uv})p(d_{uw})p(d_{vw})$, respectively. This requires link independence assumption, which is not true, however, correlations are expectedly diminished due to averaging processes (like in mean field calculations [74]). In this way, the local clustering coefficient is formulated as

$$cl(r_u) = \frac{\delta^2 \int_{r_w=0}^{R} \int_{r_v=0}^{R} \int_{\psi=0}^{2\pi} \int_{\phi=0}^{2\pi} p(d_{uv})p(d_{uw})p(d_{vw}) \mathrm{d}\phi \mathrm{d}\psi \sinh(r_v) \sinh(r_w) \mathrm{d}r_v \mathrm{d}r_w}{\delta^2 \int_{r_w=0}^{R} \int_{r_v=0}^{R} \int_{\psi=0}^{2\pi} \int_{\phi=0}^{2\pi} p(d_{uv})p(d_{uw}) \mathrm{d}\phi \mathrm{d}\psi \sinh(r_v) \sinh(r_w) \mathrm{d}r_v \mathrm{d}r_w} \ . \tag{31}$$

For estimating these integrals in the numerator and the denominator the following functions are defined:

$$\int_{\psi=0}^{2\pi}\int_{\phi=0}^{2\pi} p(d_{uv})p(d_{uw})p(d_{vw})\mathrm{d}\phi\mathrm{d}\psi \approx \tag{32}$$
$$\approx \int_{\psi=0}^{2\pi}\int_{\phi=0}^{2\pi} \exp\left(-x\sin\frac{\phi}{2} - y\sin\frac{\psi}{2} - z\sin\frac{|\psi-\phi|}{2}\right)\mathrm{d}\phi\mathrm{d}\psi =: \mathrm{Nu}(x,y,z)$$

and

$$\int_{\psi=0}^{2\pi}\int_{\phi=0}^{2\pi} p(d_{uv})p(d_{uw})\mathrm{d}\phi\mathrm{d}\psi \approx \int_{\psi=0}^{2\pi}\int_{\phi=0}^{2\pi} \exp\left(-x\sin\frac{\phi}{2} - y\sin\frac{\psi}{2}\right)\mathrm{d}\phi\mathrm{d}\psi =: \mathrm{De}(x,y) \tag{33}$$

where the general connection probability formula (16), the approximation $e^{\frac{d_{uv}}{2}} \approx e^{\frac{r_u+r_v}{2}}\sqrt{\frac{1-\cos\phi}{2}}$ are applied and

$$x = \frac{8}{\bar{k}}\delta e^{\frac{r_u+r_v}{2}} \ , \ y = \frac{8}{\bar{k}}\delta e^{\frac{r_u+r_w}{2}} \ , \ z = \frac{8}{\bar{k}}\delta e^{\frac{r_v+r_w}{2}} \ . \tag{34}$$

Now we apply asymptotic expansions of $\mathrm{Nu}(x,y,z)$ and $\mathrm{De}(x,y)$ in order to approximate them. (Asymptotic expansion here means that x,y,z are large parameters and we are interested in the asymptotic behaviour of these integrals as $\{x,y,z\}\to\infty$). Note that $\mathrm{De}(x,y)$ is simply the product of two integrals which reads as

$$\mathrm{De}(x,y) := \int_{\psi=0}^{2\pi}\exp\left(-y\sin\frac{\psi}{2}\right)\mathrm{d}\psi\int_{\phi=0}^{2\pi}\exp\left(-x\sin\frac{\phi}{2}\right)\mathrm{d}\phi$$
$$= 4\pi^2(\mathrm{I}(0,x)-\mathrm{S}(0,x))(\mathrm{I}(0,y)-\mathrm{S}(0,y)) \approx \frac{16}{xy} \tag{35}$$

due to that $\mathrm{I}(0,x)$-$\mathrm{S}(0,x) \approx \frac{2}{\pi}x^{-1}$ based on its asymptotic expansion [71] .

For approximating $\mathrm{Nu}(x,y,z)$ we use Laplace's [75] method to generate first orders of the asymptotic expansion with respect to x,y and z. For this we take the first order Taylor series expansion of the sinus functions around 0 and 2π where the integral is dominant for larger x,y,z. Performing the double integral (32) with these series and erasing the exponentially small terms, we get the following four terms with respect to that x is in the neighbourhood of 0 or 2π and y is in the neighbourhood of 0 or 2π :

$$\mathrm{Nu}(x,y,z) \approx 2\frac{4(x+y+2z)}{(x+y)(x+z)(y+z)} + 2\frac{4}{(x+z)(y+z)} = \frac{16(x+y+z)}{(x+y)(x+z)(y+z)} \ . \tag{36}$$

Now the clustering coefficient can be written as

$$cl(r_u) \approx \frac{\frac{\delta^2}{2}\int_{r_w=0}^{R}\int_{r_v=0}^{R}\mathrm{Nu}(x,y,z)\sinh(r_v)\sinh(r_w)\mathrm{d}r_v\mathrm{d}r_w}{\frac{\delta^2}{2}\int_{r_w=0}^{R}\int_{r_v=0}^{R}\mathrm{De}(x,y,z)\sinh(r_v)\sinh(r_w)\mathrm{d}r_v\mathrm{d}r_w} \approx$$
$$\approx \frac{\int_{r_w=0}^{R}\int_{r_v=0}^{R}\frac{16(x+y+z)}{(x+y)(x+z)(y+z)}\sinh(r_v)\sinh(r_w)\mathrm{d}r_v\mathrm{d}r_w}{\int_{r_w=0}^{R}\int_{r_v=0}^{R}\frac{16}{xy}\sinh(r_v)\sinh(r_w)\mathrm{d}r_v\mathrm{d}r_w} \tag{37}$$

Based on this it can be seen that $cl(r_u)$ does NOT depend on the density parameter δ, and depends on the average degree $\bar{k}$ only through $r_u(k,\bar{k})$ (see equation (20)) because all the x,y,z terms

contain a $\frac{8}{k}\delta$ factor. In this way both integrals in the numerator and denominator posses a $\frac{1}{\delta^2}$ factor. (Note, that both the numerator and denominator are independent from δ).

In what follows we explore how the local clustering coefficient of a node is depending on the expected degree k. This is possible to perform through the inverse function of $\bar{k}(r_u)$ (based on (20)) which is $r_u(k) = R - 2\ln\left(2k/\bar{k}\right)$. First the denominator is calculated which is possible in a parametric way.

$$\int_{r_w=0}^{R}\int_{r_v=0}^{R}\frac{16}{xy}\sinh(r_v)\sinh(r_w)\mathrm{d}r_v\mathrm{d}r_w = \frac{1}{9}e^{-4R}(1-4e^{3R/2}+3e^{2R})^2k^2 \approx k^2 \tag{38}$$

with the substitutions x, y in (34) and $r_u(k)$ above. (The term $\frac{16}{xy}$ does not depend on $\bar{k}$ due to the x, y and $r_u(k)$ substitution). Note that this is a good cross-validation of this formula, because the expected number of link pairs of a node with given expected degree k is approximately $k(k-1)/2 \approx k^2/2$. This is because if the node degree κ has Poisson distribution with parameter k then the expected number of link pairs at this node is $E\left[\frac{\kappa(\kappa-1)}{2}\right] = \sum_{l=0}^{\infty}\frac{l(l-1)}{2}\frac{k^l}{l!}e^{-l}$, which is exactly $\frac{k^2}{2}$. Based on the equations (37), (38) and substituting x, y, z into the formula of the integrand one can obtain

$$cl(k,\bar{k},R) \approx \int_{r_w=0}^{R}\int_{r_v=0}^{R}\frac{\bar{k}e^{\frac{1}{2}(r_v+r_w-R)}\left(\bar{k}e^{\frac{1}{2}(r_v+R)}+\bar{k}e^{\frac{1}{2}(r_w+R)}+2ke^{\frac{1}{2}(r_v+r_w)}\right)}{4\left(e^{\frac{r_v}{2}}+e^{\frac{r_w}{2}}\right)\left(e^{R/2}\bar{k}+2ke^{\frac{r_v}{2}}\right)\left(e^{R/2}\bar{k}+2ke^{\frac{r_w}{2}}\right)}\mathrm{d}r_v\mathrm{d}r_w \ . \tag{39}$$

This double integral on the right hand side can be assessed symbolically by substitution, but even a simplified result is still quite spacious (see the next note). Nevertheless, the detailed analysis of this function reveals that it is approximately independent of R, and as k is increasing, the local clustering coefficient tends to

$$cl(k,\bar{k}) \approx \ln(2)\bar{k}k^{-1} \ . \tag{40}$$

For simplicity and for catching the behaviour of $cl(k,\bar{k})$ even for smaller k values, the following intuitive form of approximation is calculated by numerical matching. The intuition is based on the observation that the integrand itself is in the form of a fraction of a first order and a second order polynomial of k.

$$\int_{r_w=0}^{R}\int_{r_v=0}^{R}\frac{\bar{k}e^{\frac{1}{2}(r_v+r_w-R)}\left(\bar{k}e^{\frac{1}{2}(r_v+R)}+\bar{k}e^{\frac{1}{2}(r_w+R)}+2ke^{\frac{1}{2}(r_v+r_w)}\right)}{4\left(e^{\frac{r_v}{2}}+e^{\frac{r_w}{2}}\right)\left(e^{R/2}\bar{k}+2ke^{\frac{r_v}{2}}\right)\left(e^{R/2}\bar{k}+2ke^{\frac{r_w}{2}}\right)}\mathrm{d}r_v\mathrm{d}r_w \ \approx \frac{1+ak}{b+ck+dk^2} \tag{41}$$

where the coefficient a, b, c, d are approximately independent of R and is depending only on $\bar{k}$. The coefficient is summarised in the Table 3 for three cases: for the lower bound of the average degree 1, for the upper bound 4, and $\bar{k} = 2.27$ which latter average degree comes from the numerical simulation of the network formation game.

Note that, for larger k's

$$\frac{1+ak}{b+ck+dk^2} \approx \frac{a}{d}k^{-1} \ , \ \frac{1}{2}\bar{k} \le k \le \frac{1}{2}\bar{k}e^{\frac{R}{2}} \ , \tag{42}$$

and $\frac{a}{d}$ is very close to $\ln(2)\bar{k}$ for all the three cases, as expected.

$\bar{k}$	a	b	c	d
1	0.598	1.008	2.168	0.869
2.27	0.331	1.002	1.019	0.209
4	0.220	1.002	0.618	0.080

Table 3: The clustering coefficient as a function of the average degree.

It is now possible to compute average clustering based on the approximation above as

$$cl = \int_{k=\frac{1}{2}\bar{k}}^{\frac{1}{2}\bar{k}e^{\frac{R}{2}}} cl(k,\bar{k})\frac{\partial}{\partial k}(1-\bar{F}(k))\mathrm{d}k \approx \int_{k=\frac{1}{2}\bar{k}}^{\frac{1}{2}\bar{k}e^{\frac{R}{2}}} \frac{1+ak}{b+ck+dk^2}\frac{\bar{k}^2}{2k^3}\mathrm{d}k \ . \tag{43}$$

Evaluating this integral for the average degree lower bound $\bar{k} = 1$, upper bound $\bar{k} = 4$, and the average degree in simulations $\bar{k} = 2.27$, we obtain, using Table 3, $cl = 0.447075, 0.447615, 0.447146$, respectively. We have also performed more extensive numerical experiments showing that average clustering does not significantly depend on the average degree for $\delta \in [10^{-8}, 10^{-2}]$ and $R \in [10, 20]$. Its dependence on R is also negligible, which is not surprising since R appears only on the upper limit of the integral, and this upper limit negligibly affects the result since the integrands decrease as $\sim k^{-5}$. All these analytic and numeric results are in a good agreement with simulations, see Figure 15.

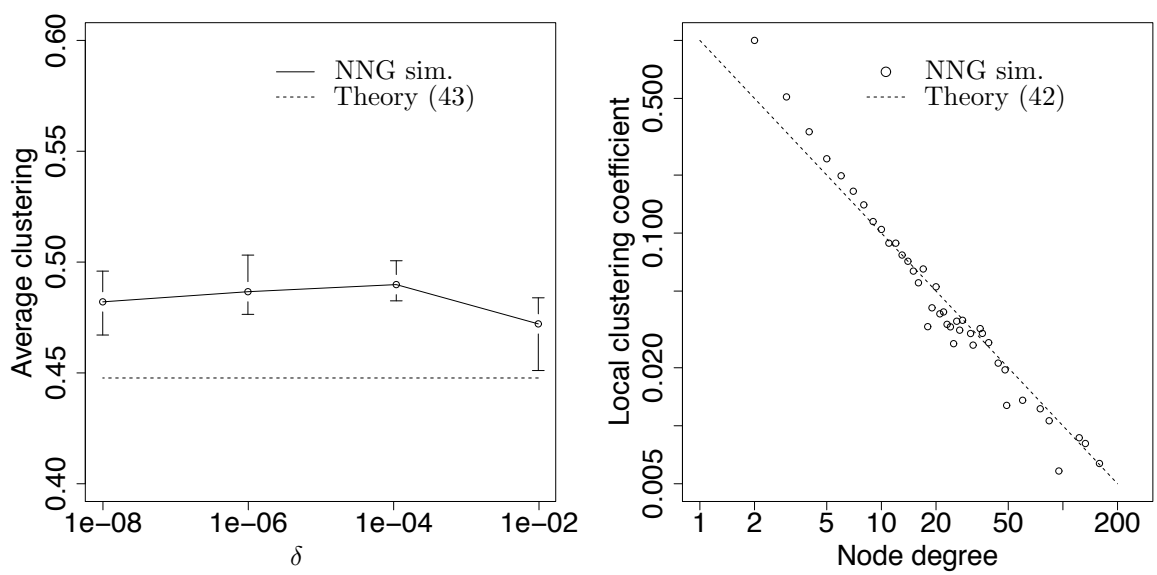

Figure 15: Average clustering as a function of δ, and local clustering as a function of node degree.

Appendix 8 - Evaluating the integral (39)

The integral for computing the local clustering coefficient presented (39) can be evaluated by

the following substitution

$$\xi = \mathrm{Exp}\left(\frac{r_v}{2}\right) \ , \ \zeta = \mathrm{Exp}\left(\frac{r_w}{2}\right) \ , \ \mathrm{d}\xi = \mathrm{Exp}\left(\frac{r_v}{2}\right)\frac{1}{2}\mathrm{d}r_v \ , \ \mathrm{d}\zeta = \mathrm{Exp}\left(\frac{r_w}{2}\right)\frac{1}{2}\mathrm{d}r_w \ , \tag{44}$$

which is in the form

$$cl(k,\bar{k},R) \approx \int_1^{e^{\frac{R}{2}}}\int_1^{e^{\frac{R}{2}}} \frac{e^{-\frac{R}{2}}\bar{k}\left(e^{\frac{R}{2}}\bar{k}(\zeta+\xi)+2\zeta k\xi\right)}{(\zeta+\xi)\left(e^{\frac{R}{2}}\bar{k}+2\zeta k\right)\left(e^{\frac{R}{2}}\bar{k}+2k\xi\right)}\mathrm{d}\xi\mathrm{d}\zeta \ . \tag{45}$$

A simplified version of the result of the integral (39) is

$$\begin{aligned}
&\frac{1}{8k^2}\Bigg(e^{-\frac{R}{2}}\Bigg(\bar{k}e^{R/2}\Bigg(\bar{k}\Bigg(\mathrm{Li}_2\left(\frac{2\left(1+e^{-\frac{R}{2}}\right)k}{2k-\bar{k}}\right)-\mathrm{Li}_2\left(\frac{2\left(1+e^{-\frac{R}{2}}\right)k}{2k+\bar{k}}\right)+\\
&\mathrm{Li}_2\left(-\frac{2\left(1+e^{R/2}\right)k}{e^{R/2}\bar{k}-2k}\right)+\mathrm{Li}_2\left(\frac{4k}{2k+e^{R/2}\bar{k}}\right)-\mathrm{Li}_2\left(\frac{2\left(1+e^{R/2}\right)k}{2k+e^{R/2}\bar{k}}\right)-\mathrm{Li}_2\left(\frac{4k}{2k-e^{R/2}\bar{k}}\right)-\\
&\mathrm{Li}_2\left(-\frac{4k}{\bar{k}-2k}\right)+\mathrm{Li}_2\left(\frac{4k}{2k+\bar{k}}\right)\Bigg)+\bar{k}\Bigg(\log\left(e^{R/2}+1\right)\Bigg(\ln\left(-\frac{2ke^{-\frac{R}{2}}+\bar{k}}{2k-\bar{k}}\right)-\ln\left(\frac{\bar{k}-2ke^{-\frac{R}{2}}}{2k+\bar{k}}\right)+\\
&\ln\left(\frac{e^{R/2}(2k+\bar{k})}{\bar{k}e^{R/2}-2k}\right)-\ln\left(\frac{e^{R/2}(\bar{k}-2k)}{2k+\bar{k}e^{R/2}}\right)\Bigg)+\ln\left(2e^{R/2}\right)\left(\ln\left(1-\frac{4k}{2k+\bar{k}}\right)-\ln\left(\frac{4k}{\bar{k}-2k}+1\right)\right)+\\
&\ln(2)\left(\ln\left(1-\frac{4k}{2k+\bar{k}e^{R/2}}\right)-\ln\left(\frac{4k}{\bar{k}e^{R/2}-2k}+1\right)\right)+2\Bigg(\ln\left(e^{R/2}(2k+\bar{k})\right)-\\
&\ln\left(2k+\bar{k}e^{R/2}\right)\Bigg)\left(\tanh^{-1}\left(\frac{2k}{\bar{k}}\right)-\tanh^{-1}\left(\frac{2ke^{-\frac{R}{2}}}{\bar{k}}\right)\right)\Bigg)+8k\left(\ln\left(e^{R/2}\right)-\ln\left(e^{R/2}+1\right)+\ln(2)\right)\Bigg)+\\
&4k\bar{k}\left(\ln(4)-2\ln\left(e^{R/2}+1\right)\right)\Bigg)\Bigg) \ ,
\end{aligned} \tag{46}$$

where the function $\mathrm{Li}_2(z)=\sum_{k=1}^{\infty}\frac{z^k}{k^2}$ is the di-logarithm special function. We observe that factors $\mathrm{Exp}(-R/2)$ and $\mathrm{Exp}(R/2)$ appear in several terms. If R is sufficiently large, e.g., ranging between realistic values of 10 and 20, then we can neglect the exponentially smaller terms, keeping only the exponentially large dominating terms. For example,

$$\frac{\bar{k}-2ke^{-\frac{R}{2}}}{2k+\bar{k}} \approx \frac{\bar{k}}{2k+\bar{k}} \quad \text{and} \quad \frac{e^{R/2}(2k+\bar{k})}{\bar{k}e^{R/2}-2k} \approx \frac{2k+\bar{k}}{\bar{k}} \ . \tag{47}$$

Using this procedure, after some simplifications, we finally obtain an $R-$free expression for clus-

tering:

$$cl(k,\bar{k}) \approx \frac{1}{8k^2}\bar{k}\left(8k\ln(2) + \bar{k}\left(\ln\left(\frac{\bar{k}+2k}{\bar{k}}\right)\ln\left(\frac{\bar{k}+2k}{\bar{k}-2k}\right) + \ln(2)\ln\left(\frac{\left(\bar{k}-2k\right)^2}{\left(\bar{k}+2k\right)^2}\right)\right) + \right.$$
$$\bar{k}\left(\mathrm{Li}_2\left(\frac{2k}{2k-\bar{k}}\right) + \mathrm{Li}_2\left(-\frac{2k}{\bar{k}}\right) - \mathrm{Li}_2\left(\frac{2k}{\bar{k}}\right) - \right.$$
$$\left.\left.\mathrm{Li}_2\left(-\frac{4k}{\bar{k}-2k}\right) - \mathrm{Li}_2\left(\frac{2k}{2k+\bar{k}}\right) + \mathrm{Li}_2\left(\frac{4k}{2k+\bar{k}}\right)\right)\right) \tag{48}$$

We can now see that $cl(k,\bar{k}) \to \ln(2)\bar{k}\ k^{-1}$ as k increases, because the logarithmic terms become zero, while the dilogarithmic terms eliminate each other. The analysis of this function at $k = 0$ also shows that $cl(0,\bar{k}) = 1$, from which it follows that $b = 1$ in the polynomial matching the numerical calculations, cf. Table 3.

Appendix 9 - Expected out-degree distribution in a frame topology with quasi-uniform node density

The radial coordinate density in case of quasi-uniform node density is

$$\rho(r,\alpha) := \frac{\alpha\sinh(\alpha r)}{\cosh(\alpha R) - 1} \approx \alpha e^{\alpha(r-R)} \tag{49}$$

while the angle density remains uniform ($\frac{1}{2\pi}$) over the range $[1, 2\pi]$. Given a point pair (u, v), first we determine the probability $p(r_u, \alpha)$ that the $u \to v$ link exists, then based on this the average out degree $k(r_u, \alpha)$ of u is calculated, and finally $\bar{F}(k, \alpha)$ is also given.

Probability $p(r_u, \alpha)$ is equal to the probability that none of the remaining $N - 2$ points fall in the intersection of the v-centred d_{uv} circle and the R-disk. Let us denote by p_1 the probability that a point whose coordinates generated by randomly according to the densities above falls inside the intersection. Using p_1 the probability $p(r_u, \alpha)$ can be calculated and approximated as

$$p(r_u,\alpha) = (1-p_1)^{N-2} \approx e^{-Np_1} \tag{50}$$

The calculation of p_1 can be performed by using the node density function in the following way [72]

$$p_1 = \int_0^{\max(0,d-r_v)} \rho(r,\alpha)\mathrm{d}r + \frac{1}{2\pi}\int_{|d-r_v|}^{\min(R,d+r_v)} \rho(r,\alpha)2\theta(r)\mathrm{d}r \tag{51}$$

where

$$\theta(r) = \arccos\frac{\cosh r_v \cosh r - \cosh d}{\sinh r_v \sinh r}\ . \tag{52}$$

In [72] a useful approximation is presented for quite similar integrals, based on which one can write

$$p_1 \approx \frac{4e^{\frac{1}{2}(d-R-r_v)}\alpha}{\pi(-1+2\alpha)} \tag{53}$$

for $0.5 < \alpha \leq 1$.

Now the expected out-degree of u can be written as

$$k_{\text{out}}(r_u, \alpha) \approx \frac{N}{2\pi} \int_0^R \int_0^{2\pi} e^{-Np_1} \mathrm{d}\phi \rho(r_v) \mathrm{d}r_v \ . \tag{54}$$

Using the approximation of p_1 and $\cosh(d/2) \approx e^{\frac{r_u+r_v}{2}} \sin\frac{\phi}{2}$ one can formulate

$$\int_0^{2\pi} e^{-Np_1} \mathrm{d}\phi \approx \int_0^{2\pi} e^{-x \sin\frac{\phi}{2}} \mathrm{d}\phi \approx 2\pi(\mathrm{I}(0,x) - \mathrm{S}(0,x)) \approx \frac{4}{x} \tag{55}$$

where

$$x = 4\frac{N}{\pi}\frac{\alpha}{2\alpha - 1} e^{\frac{r_u - R}{2}} \ . \tag{56}$$

Note, that x does not depend on r_v, therefore the second integration by r_v results

$$k_{\text{out}}(r_u, \alpha) \approx \frac{N}{2\pi}\frac{4}{x} \int_0^R \rho(r_v, \alpha) \mathrm{d}r_v = \frac{2\alpha - 1}{2\alpha} e^{\frac{R}{2}} e^{-\frac{r_u}{2}} \ . \tag{57}$$

Note, that for $\alpha = 1$ we get back the result for the uniform density case, (20).

Now the (approximation of the) complement cumulative distribution function $\bar{F}(k)$ can be derived as,

$$\bar{F}(k) = \int_0^{r_u(k)} \rho(r, \alpha) \mathrm{d}r \approx e^{\alpha(r_u(k) - R)} = \left(\frac{1 - \frac{1}{2\alpha}}{k} \right)^{2\alpha} \tag{58}$$

where $r_u(k)$ is the inverse function of $k_{\text{out}}(r_u)$. The simulation results displayed in Figure 16 readily confirm this finding.

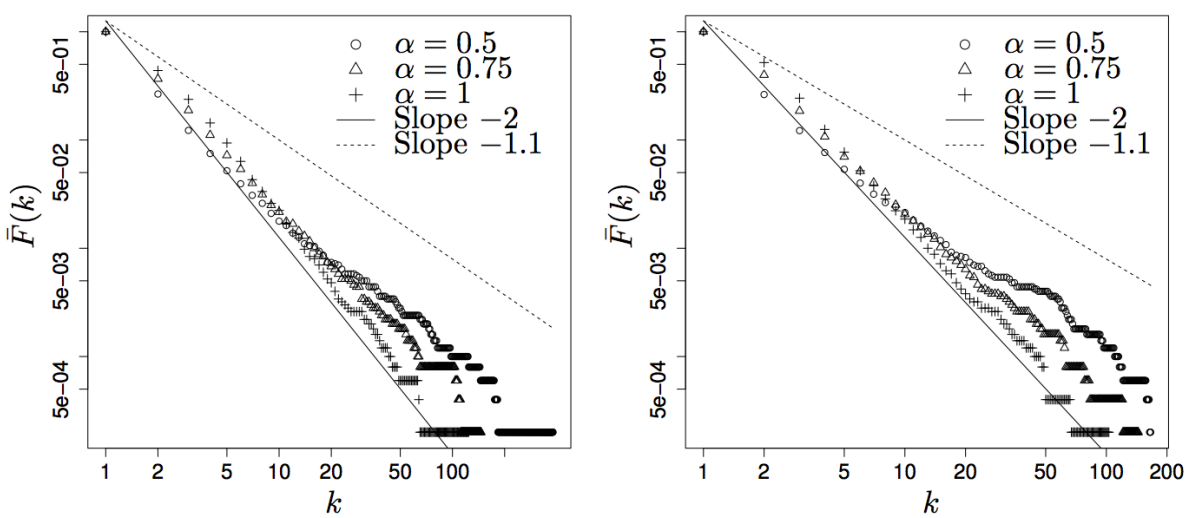

Figure 16: The in and out degree distributions of the NNG for various settings of the α parameter.

Appendix 10 - Statistical Significance

In this note we provide probability estimates which represent the statistical significance of that the NNG equilibrium network links' containment by the real networks is very unlikely to occur by random chance, but rather is likely to be attributable to the specific characteristics of our embedding and NNG processes.

The NNG equilibrium network (graph) is a transformation of the real network under investigation by an embedding and a gaming (NNG) process. Although this transformation is completely deterministic, the statistical significance test can be performed in the following two ways: In the first approach the NNG equilibrium network is substituted by a completely random network with the same average degree $\bar{k}_{\mathrm{NNG}}$, that is $\frac{N}{2}\bar{k}_{\mathrm{NNG}}$ links are randomly chosen from the possible $\frac{N(N-1)}{2}$ number of links. The probability that p fraction of these links (e.g. $p = 0.83$) are contained by the real network (having $\frac{N}{2}\bar{k}$ links) can be calculated as

$$\frac{\binom{N(N-1)/2-N/2\bar{k}}{(1-p)N/2\bar{k}_{\mathrm{NNG}}}\binom{N/2\bar{k}}{pN/2\bar{k}_{\mathrm{NNG}}}}{\binom{N(N-1)/2}{N/2\bar{k}_{\mathrm{NNG}}}} \tag{59}$$

which is in the order of $O(e^{-N})$. Because this probability is extremely small for reasonable N, our result is very unlikely to occur also along with fully random networks with fixing only the number of edges. For example, taking the values on the Internet AS-level topology embedding ($N = 4919, \frac{N}{2}\bar{k} = 28361, \frac{N}{2}\bar{k}_{\mathrm{NNG}} = 5490, p = 0.83$) the probability above is 5.62×10^{-11068}.

A more refined randomization of the NNG equilibrium network is to substitute only the embedding process by fully random generation of H2 coordinates (with such coordinate distribution similar to the one resulted by the embedding process) and then apply the gaming process (as if the embedding was wrong and had no concern to the original real network). In this way, the resulted random NNG network preserves not only the average degree, but the degree distribution and also the clustering coefficient of the original NNG equilibrium network. Let X be a random variable denoting the number of links from the randomized NNG equilibrium network contained by the original real network. Inevitably, X is a non-negative random variable bounded also from above by $P := \frac{N}{2}\bar{k}_{\mathrm{NNG}}$. Although the exact distribution of X cannot be calculated due to the dependent link establishment of the gaming process, the expected value of X (which is insensitive to link dependence) is

$$E(X) = \frac{N}{2}\bar{k}\frac{\frac{N}{2}\bar{k}_{\mathrm{NNG}}}{\frac{N(N-1)}{2}} \approx \frac{1}{2}\bar{k}_{\mathrm{NNG}}\,\bar{k}. \tag{60}$$

Based on this average value, a conservative upper bound can also be given on the probability that the level of this link containment exceeds a certain threshold $0 < C < P$. Applying Hoeffding's inequality [76] we can state that

$$P(X > C) \leq \left(\frac{E(X)}{C}\right)^{\frac{C}{P}} \left(\frac{P - E(X)}{P - C}\right)^{1-\frac{C}{P}} \tag{61}$$

This upper bound is far below 0.05 for several reasonable $\bar{k}$ and N. For example, the probability that more than 83 percent of the randomized NNG equilibrium network links (C =4556 of the total 5490 edges) coincide Internet real edges (among the total 28 361) is upper bounded by 0.00136044.

The complement of the upper bound of the probability above (1-upper bound) can also be considered as a weight of our statement (in the example above 0.99864).

Appendix 11 - Euclidean plane

In this note we analyze the degree distribution in NNG equilibrium networks constructed on sets of points sprinkled uniformly at random over Euclidean disks. We show that the expected degree of a node located in the disk centre is around 1, while the expected degree of a node at the disk boundary is around 1/2. In view of this lack of variability of node degrees, the degree distribution in the Euclidean case cannot have any fat tails.

According to (7) the expected degree of a node u is

$$\delta \int_0^R \int_0^{2\pi} e^{-\delta T_{uv}} \mathrm{d}\phi r_v \mathrm{d}r_v \ , \tag{62}$$

where $\delta = N/T_R = \frac{N}{R^2\pi}$. To give an upper bound we will give a lower bound for T_{uv}. If u is the centre of the disk, then T_{uv} is the area of the intersection of the disk and an circle around v with radius r_v. If $r_v \leq R/2$, then this intersection is the circle itself around v, else the intersection contains a circle with radius $R/2$, hence

$$\begin{aligned} k(0) \leq \delta \int_0^{R/2} \int_0^{2\pi} e^{-\delta r_v^2 \pi} \mathrm{d}\phi r_v \mathrm{d}r_v + \delta \int_{R/2}^{R} \int_0^{2\pi} e^{-\delta (R/2)^2 \pi} \mathrm{d}\phi r_v \mathrm{d}r_v \\ \leq 1 - e^{-\frac{1}{4}\delta R^2 \pi} + \frac{3}{4}\delta R^2 \pi e^{-\frac{1}{4}\delta R^2 \pi} \leq 1 + 3\frac{N}{4} e^{-N/4} \leq 1 + \frac{3}{e}. \end{aligned} \tag{63}$$

Moreover, if $N \geq 6$ then $k(0) \leq 1.05$

To give a lower bound to the expected degree we will count with the whole circle around v instead of the intersection:

$$k(0) \geq \delta \int_0^R \int_0^{2\pi} e^{-\delta r_v^2 \pi} \mathrm{d}\phi r_v \mathrm{d}r_v = \delta 2\pi \int_0^R e^{-\delta r_v^2 \pi} r_v \mathrm{d}r_v = 1 - e^{-\delta R^2 \pi} = 1 - e^{-N}. \tag{64}$$

If $N \geq 6$, then $k(0) \geq 0.99$.

Similarly, for the expected degree of a node u at the disk boundary

$$k(R) \geq \delta \int_0^R \int_0^{2\pi} e^{-\delta d^2 \pi} \mathrm{d}\phi r_v \mathrm{d}r_v, \tag{65}$$

where d is the distance between u and v, and according to the cosines law, $d^2 = R^2 + r_v^2 - 2Rr_v \cos\phi_v$. The inner integration is

$$\int_0^{2\pi} e^{-\delta\pi(R^2 + r_v^2 - 2r_u r_v \cos\phi_v)} \mathrm{d}\phi = 2\pi \mathrm{I}(0, 2\pi\delta r_v R) e^{-\delta\pi(R^2 + r_v^2)}, \tag{66}$$

where $\mathrm{I}(0, x)$ is the BesselI function. Unfortunately the BesselI cannot be integrated, but we can

use that $\mathrm{I}(0,x) \sim e^x/\sqrt{2\pi x}$. Hence

$$k(R) \geq \int_0^R \frac{2\pi\delta}{\sqrt{4\pi^2\delta R r_v}} e^{2\pi\delta R r_v - \delta\pi(R^2 - r_v^2)} r_v \mathrm{d}r_v = \int_0^R \frac{r_v N}{\sqrt{R^3\pi}} e^{-\pi(R-r_v)^2 N/R^2} \mathrm{d}r_v$$
$$\geq \frac{2\sqrt{N}}{3\sqrt{\pi}} \mathrm{HypergeometricPFQ}\left(\left\{\frac{1}{2}, 1\right\}, \left\{\frac{5}{4}, \frac{7}{4}\right\}, -N\right) \xrightarrow[N\to\infty]{} \frac{1}{2} \quad (67)$$

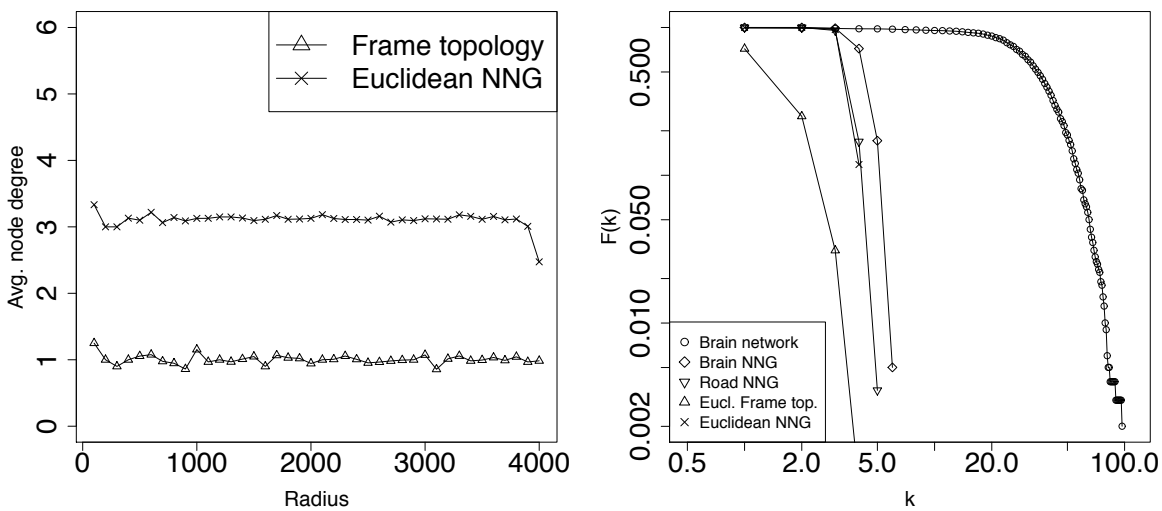

Figure 17: Average degree of nodes as a function of their radial coordinates on an Euclidean disk (left), and the cumulative distribution function of node degrees in the corresponding NNG equilibrium, its frame topology, the Hungarian road network, the brain network, and its NNG equilibrium (right).

On the left panel of Figure 17 the simulation results support the analytical findings that in the Euclidean case the expected degree nodes as a function of their radial coordinates has very low variability in the NNG equilibrium networks and their frame topologies. As a consequence of this low variability the degree distributions do not have any fat tails or power laws, and decay fast with the node degree, the right panel of Figure 17. Clustering is still relatively strong however: in the synthetic Euclidean NNG network it is 0.19, in the road NNG network it is 0.22, while in the brain network and its NNG, the clustering values are 0.46 and 0.21 respectively.

Appendix 12 - Heaviside step function approximation to the effective connection probability

The Heaviside step function with the step at

$$R' = 2\ln\frac{\bar{k}}{8\delta} \quad (68)$$

is a good approximation to the effective connection probability in Eq. (16) for $\delta \in [10^{-6}, 10^{-3}]$ and $R = [12, 18]$. With this step-function approximation, node u connects to v iff $d_{uv} \leq R'$. Therefore the expected degree of u is the expected number of points lying within the intersection of the $R-$disk and the u-centred disk of radius R'.

To see that this step function is indeed a good approximation to the effective connection probability in the NNG equilibrium, recall that the area of the two disks above can be approximated as

$$T_{R',R} = 4e^{\frac{R'}{2}} e^{\frac{R-r_u}{2}}. \tag{69}$$

From these one can obtain

$$k_{\text{out}}(r_u) \approx N \frac{T_{R',R}}{T_{R-\text{disk}}} = N \frac{4e^{\frac{R'}{2}} e^{\frac{R-r_u}{2}}}{\pi e^R} \ . \tag{70}$$

If R' from (68) is substituted into the formula above we get back the expected out-degree in (20). In particular, if $R' = R$ (as in [77]), then

$$k_{\text{out}}(r_u) = \frac{4}{\pi} N e^{-\frac{r_u}{2}} \tag{71}$$

and

$$\bar{k} = \frac{8}{\pi} N e^{-\frac{R}{2}}, \tag{72}$$

which coincides with Eqs. (12,13) in [77].

Appendix 13 - Nonnavigable network example

One cannot expect every real network to be highly navigable because navigation is not an important function of every real network. Here we consider one example, the Pretty-Good-Privacy (PGP) web of trust network, specifically the December 2006 snapshot and its hyperbolic coordinates from [78]. These data are then processed exactly as for all the other networks in the main text. However, as expected, the navigation success ratio and precision metrics reported for this network in Table 4 are substantially lower than for the navigable networks in the main text.

	PGP
Nodes	4899
Real edges ($\|R\|$)	67650
NNG edges ($\|M\|$)	29311
True positives ($\|T\|$)	6945
False positives ($\|F\|$)	22366
Precision ($\|T\|/\|M\|$)	24%
Navigation success ratio	36%

Table 4: The table quantifies the relevant edge statistics showing the total number of edges in the core of the PGP network $|R|$, and in its NNG equilibrium network $|M|$, the number of true positive edges $|T|= |M \cap R|$, the number of false positive green edges $|F|= |M \setminus R|$, and the true positive rate, or precision, defined as $|T|/|M|$.

References

[1] Barrat, A., Barthelemy, M. & Vespignani, A. *Dynamical processes on complex networks*, vol. 1 (Cambridge University Press Cambridge, 2008).

[2] Kitsak, M. *et al.* Identification of influential spreaders in complex networks. *Nat. Phys.* **6**, 888–893 (2010).

[3] Watts, D. J., Dodds, P. S. & Newman, M. E. J. Identity and search in social networks. *Science* **296**, 1302 (2002).

[4] Pastor-Satorras, R. & Vespignani, A. Epidemic spreading in scale-free networks. *Phys. Rev. Lett.* **86**, 3200 (2001).

[5] Rhodes, C. J. & Anderson, R. M. Power laws governing epidemics in isolated populations. *Nature* **381**, 600–602 (1996).

[6] Ferguson, N. Capturing human behaviour. *Nature* **446**, 733–733 (2007).

[7] Doerr, C., Blenn, N. & Van Mieghem, P. Lognormal infection times of online information spread. *PloS ONE* **8**, e64349 (2013).

[8] Meloni, S., Arenas, A. & Moreno, Y. Traffic-driven epidemic spreading in finite-size scale-free networks. *Proc. Natl. Acad. Sci. USA* **106**, 16897–16902 (2009).

[9] Barthélemy, M., Barrat, A., Pastor-Satorras, R. & Vespignani, A. Velocity and hierarchical spread of epidemic outbreaks in scale-free networks. *Phys. Rev. Lett.* **92**, 178701 (2004).

[10] Miritello, G., Moro, E. & Lara, R. Dynamical strength of social ties in information spreading. *Phys. Rev. E* **83**, 045102 (2011).

[11] Gallos, L. K., Song, C., Havlin, S. & Makse, H. A. Scaling theory of transport in complex biological networks. *Proc. Natl. Acad. Sci. USA* **104**, 7746–7751 (2007).

[12] Moreno, Y., Nekovee, M. & Pacheco, A. F. Dynamics of rumor spreading in complex networks. *Phys. Rev. E* **69**, 066130 (2004).

[13] Barabási, A.-L. & Oltvai, Z. N. Network biology: understanding the cell's functional organization. *Nat. Rev. Genet.* **5**, 101–13 (2004).

[14] Yamada, T. & Bork, P. Evolution of biomolecular networks: lessons from metabolic and protein interactions. *Nat. Rev. Mol. Cell. Bio.* **10**, 791–803 (2009).

[15] Bullmore, E. & Sporns, O. Complex Brain Networks: Graph Theoretical Analysis of Structural and Functional Systems. *Nat. Rev. Neurosci.* **10**, 168–198 (2009).

[16] Chialvo, D. Emergent complex neural dynamics. *Nat. Phys.* **6**, 744–750 (2010).

[17] Milgram, S. The Small World Problem. *Psychol. Today* **1**, 61–67 (1967).

[18] Travers, J. & Milgram, S. An Experimental Study of the Small World Problem. *Sociometry* **32**, 425–443 (1969).

[19] Kleinberg, J. Navigation in a small world. *Nature* **406**, 845–845 (2000).

[20] Dodds, P. S., Muhamad, R. & Watts, D. J. An experimental study of search in global social networks. *Science* **301**, 827–9 (2003).

[21] Liben-Nowell, D., Novak, J., Kumar, R., Raghavan, P. & Tomkins, A. Geographic Routing in Social Networks. *Proc. Natl. Acad. Sci. USA* **102**, 11623–11628 (2005).

[22] Simsek, O. & Jensen, D. Navigating networks by using homophily and degree. *Proc. Natl. Acad. Sci. USA* **105**, 12758–62 (2008).

[23] Boguñá, M., Krioukov, D. & Claffy, K. Navigability of Complex Networks. *Nat. Phys.* **5**, 74–80 (2009).

[24] Caretta Cartozo, C. & De Los Rios, P. Extended Navigability of Small World Networks: Exact Results and New Insights. *Phys. Rev. Lett.* **102**, 238703 (2009).

[25] Hu, Y., Wang, Y., Li, D., Havlin, S. & Di, Z. Possible Origin of Efficient Navigation in Small Worlds. *Phys. Rev. Lett.* **106**, 108701 (2011).

[26] Lee, S. H. & Holme, P. Exploring Maps with Greedy Navigators. *Phys. Rev. Lett.* **108**, 128701 (2012).

[27] Lee, S. H. & Holme, P. Geometric properties of graph layouts optimized for greedy navigation. *Phys. Rev. E* **86**, 067103 (2012).

[28] Yang, Zhi & Chen, Wei A Game Theoretic Model for the Formation of Navigable Small-World Networks. *In Proc. of the 24th International Conference on World Wide Web*, 1329–1339 (2015).

[29] Capitán, J. A. *et al.* Local-based semantic navigation on a networked representation of information. *PLoS ONE* **7**, e43694 (2012).

[30] Cornelius, S. P., Lee, J. S. & Motter, A. E. Dispensability of Escherichia coli's latent pathways. *Proc. Natl. Acad. Sci. USA* **108**, 3124–9 (2011).

[31] Nisan, N. *Algorithmic game theory* (Cambridge Universiy Press, 2007).

[32] Fabrikant, A., Luthra, A., Maneva, E., Papadimitriou, C. H. & Shenker, S. On a network creation game. In *Proc. of PODC'03*, 347–351 (2003).

[33] Anshelevich, E. *et al.* The price of stability for network design with fair cost allocation. In *Proc. of FOCS'04*, 295–304 (2004).

[34] Corbo, J. & Parkes, D. The price of selfish behavior in bilateral network formation. In *Proc. of PODC'05*, 99–107 (2005).

[35] Albers, S., Eilts, S., Even-Dar, E., Mansour, Y. & & Roditty, L. On nash equilibria for a network creation game. In *Proc. of SODA'06*, 89–98 (2006).

[36] Demaine, E. D., Hajiaghayi, M., Mahini, H. & Zadimoghaddam, M. The price of anarchy in network creation games. In *Proc. of PODC '07*, 292–298 (2007).

[37] Mihalák, M. & Schlegel, J. The price of anarchy in network creation games is (mostly) constant. *Alg. Game Theory* 276–287 (2010).

[38] Lee, S. H. & Holme, P. A greedy-navigator approach to navigable city plans. *Eu. Phys. Journ. Spec. Top.* **215**, 135–144 (2013).

[39] Papadimitriou, C. H. & Ratajczak, D. On a conjecture related to geometric routing. *Theor. Comput. Sci.* **344**, 3–14 (2005).

[40] Papadopoulos, F., Kitsak, M., Serrano, M. A., Boguñá, M. & Krioukov, D. Popularity versus similarity in growing networks. *Nature* **489**, 537–540 (2012).

[41] Penrose, M. *Random Geometric Graphs* (Oxford University Press, Oxford, 2003).

[42] Krioukov, D., Papadopoulos, F., Kitsak, M., Vahdat, A. & Boguñá, M. Hyperbolic Geometry of Complex Networks. *Phys. Rev. E* **82**, 36106 (2010).

[43] Garfinkel, R. S. & Nemhauser, G. L. *Integer programming*, vol. 4 (Wiley New York, 1972).

[44] Boguñá, M. & Pastor-Satorras, R. Class of Correlated Random Networks with Hidden Variables. *Phys. Rev. E* **68**, 36112 (2003).

[45] Newman, M. E. J. Power Laws, Pareto Distributions and Zipf's Law. *Contemp. Phys.* **46**, 323–351 (2005).

[46] Cohen, R. & Havlin, S. Scale-free networks are ultrasmall. *Phys. Rev. Lett.* **90**, 058701 (2003).

[47] Tiesinga, P. H. E., Fellous, J. M., José, J. V. & Sejnowski, T. J. Optimal information transfer in synchronized neocortical neurons. *Neurocomputing* **38-40**, 397–402 (2001).

[48] Laughlin, S. B. & Sejnowski, T. J. Communication in neuronal networks. *Science* **301**, 1870–1874 (2003).

[49] Heuvel, M. P. V. D., Kahn, R. S., Goñi, J., Sporns, O. & van den Heuvel, M. P. Brain Communication. *Proc. Natl. Acad. Sci. USA* **109**, 11372–77 (2012).

[50] Goñi, J. *et al.* Resting-brain functional connectivity predicted by analytic measures of network communication. *Proc. Natl. Acad. Sci. USA* **111**, 833–8 (2014).

[51] Szabó, D. & Gulyás, A. Notes on the topological consequences of BGP policy routing on the Internet AS topology. In *Advances in Communication Networking*, 274–281 (Springer Berlin Heidelberg, 2013).

[52] D'Souza, R. M., Borgs, C., Chayes, J. T., Berger, N. & Kleinberg, R. D. Emergence of tempered preferential attachment from optimization. *Proc. Natl. Acad. Sci. USA* **104**, 6112–6117 (2007).

[53] Muchnik, L. *et al.* Origins of power-law degree distribution in the heterogeneity of human activity in social networks. *Sci. Rep.* **3**, 1783 (2013).

[54] Krioukov, D. & Ostilli, M. Duality between equilibrium and growing networks. *Phys. Rev. E* **88**, 022808 (2013).

[55] Kleinberg, J. Navigation in a Small World. *Nature* **406**, 845 (2000).

[56] Li, G. *et al.* Towards design principles for optimal transport networks. *Phys. Rev. Lett.* **104**, 018701 (2010).

[57] Rozenfeld, H. D., Song, C. & Makse, H. A. Small-world to fractal transition in complex networks: a renormalization group approach. *Phys. Rev. Lett.* **104**, 025701 (2010).

[58] Li, G. *et al.* Optimal transport exponent in spatially embedded networks. *Phys. Rev. E* **87**, 042810 (2013).

[59] Newman, M. E. J. The Structure and Function of Complex Networks. *SIAM Rev.* **45**, 167–256 (2003).

[60] Boccaletti, S., Latora, V., Moreno, Y., Chavez, M. & Hwanga, D.-U. Complex Networks: Structure and Dynamics. *Phys. Rep.* **424**, 175–308 (2006).

[61] Ferrer i Cancho, R. & Sole, R. The small world of human language. *Proc. R. Soc. Lond. B, Biological Sciences* **268**, 2261–2265 (2001).

[62] Choudhury, M. & Mukherjee, A. The structure and dynamics of linguistic networks. In *Dynamics on and of complex networks*, 145–166 (Springer, 2009).

[63] Baronchelli, A., Ferrer i Cancho, R., Pastor-Satorras, R., Chater, N. & Christiansen, M. H. Networks in cognitive sciences. *Trends in Cognitive Sciences* **17**, 348–360 (2013).

[64] Boguñá, M., Papadopoulos, F. & Krioukov, D. Sustaining the Internet with Hyperbolic Mapping. *Nat. Comms.* **1**, 62 (2010).

[65] Milo, R. *et al.* Superfamilies of Evolved and Designed Networks. *Science* **303**, 1538–1542 (2004).

[66] Hagmann, P. *et al.* Mapping the structural core of human cerebral cortex. *PLoS Biol.* **6**, 1479–1493 (2008).

[67] Papadopoulos, F., Psomas, C. & Krioukov, D. Network mapping by replaying hyperbolic growth. *IEEE ACM T Netw* (2014).

[68] Watts, D. J., Dodds, P. S. & Newman, M. E. J. Identity and search in social networks. *Science* **296**, 1302 (2002).

[69] Kleinberg, J. Navigation in a small world. *Nature* **406**, 845–845 (2000).

[70] Boguna, M., Krioukov, D. & Claffy, K. C. Navigability of complex networks. *Nature Physics* **5**, 74–80 (2009).

[71] Abramovitz, M. & Stegun, I. *Handbook of Mathematical Functions* (Courier Dover Publication, 1965).

[72] Papadopoulos, F., Krioukov, D., Bogua, M. & Vahdat, A. Greedy forwarding in dynamic scale-free networks embedded in hyperbolic metric spaces. In *Proc. of IEEE Infocom*, 1–9 (IEEE, 2010).

[73] Boguna, M. Class of correlated random networks with hidden variables. *Physical Review E* **68**, 1–13 (2003).

[74] Fronczak, A., Fronczak, P. & Holyst, J. A. Mean-field theory for clustering coefficients in Barabasi-Albert networks. *Arxiv preprint arXiv:cond-mat/0306255 [cond-mat.stat-mech]* (2003).

[75] Bleistein, N. & Handelsman, R. *Asymptotic Expansions of Integrals* (Dover Publications (New York), 1986).

[76] Hoeffding, W. Probability inequalities for sums of bounded random variables. *Journal of the American Statistical Association* **58**, 13–30 (1963).

[77] Krioukov, D., Papadopoulos, F., Kitsak, M. & Vahdat, A. Hyperbolic geometry of complex networks. *Physical Review E* **82**, 036106 (2010).

[78] Papadopoulos, F., Kitsak, M., Serrano, M. A., Boguñá, M. & Krioukov, D. Popularity versus similarity in growing networks. *Nature* **489**, 537–540 (2012).